A tonic nicotinic brake controls spike timing in striatal spiny projection neurons

Lior Matityahu[1*], Jeffrey M. Malgady[2*], Meital Schirelman[1*], Yvonne Johansson[3#], Jennifer Wilking[2], Gilad Silberberg[3], Joshua A. Goldberg[1†] and Joshua L. Plotkin[2†]

[1]Department of Medical Neurobiology, Institute of Medical Research Israel–Canada, The Faculty of Medicine, The Hebrew University of Jerusalem, 9112102, Jerusalem, Israel
[2]Department of Neurobiology and Behavior, Stony Brook University School of Medicine, Stony Brook University, NY, 11794, USA
[3]Department of Neuroscience, Karolinska Institutet, 17177 Stockholm, Sweden
[#]Current Address: Sainsbury Wellcome Centre for Neural Circuits and Behaviour, University College London, London, UK

*Authors contributed equally to this work

[†]Equal corresponding authors

Impact Statement

A novel mechanism describing how tonic activation of nicotinic acetylcholine receptors can modulate the timing of striatal output by priming feed forward inhibition.

Abstract

Striatal spiny projection neurons (SPNs) transform convergent excitatory corticostriatal inputs into an inhibitory signal that shapes basal ganglia output. This process is fine-tuned by striatal GABAergic interneurons (GINs), which receive overlapping cortical inputs and mediate rapid corticostriatal feedforward inhibition of SPNs. Adding another level of control, cholinergic interneurons (CINs), which are also vigorously activated by corticostriatal excitation, can disynaptically inhibit SPNs by activating α4β2 nicotinic acetylcholine receptors (nAChRs) on various GINs. Measurements of this disynaptic inhibitory pathway, however, indicate that it is too slow to compete with direct GIN-mediated feed-forward inhibition. Moreover, functional nAChRs are also present on populations of GINs that respond only weakly to phasic activation of CINs, such as parvalbumin-positive fast-spiking interneurons (PV-FSIs), making the overall role of nAChRs in shaping striatal synaptic integration unclear. Using acute striatal slices we show that upon synchronous optogenetic activation of corticostriatal projections blockade of α4β2 nAChRs shortened SPN spike latencies and increased postsynaptic depolarizations. The nAChR-dependent inhibition was mediated by downstream GABA release, and data suggest that the GABA source was not limited to GINs that respond strongly to phasic CIN activation. In particular, the observed decrease in spike latency caused by nAChR blockade was associated with a diminished frequency of spontaneous inhibitory postsynaptic currents in SPNs, a parallel hyperpolarization of PV-FSIs, and was occluded by pharmacologically preventing cortical activation of PV-FSIs. Taken together, we describe a role for tonic (as opposed to phasic) activation of nAChRs in striatal function. We conclude that tonic activation of nAChRs by CINs maintains a GABAergic brake on cortically-driven striatal output by “priming” feedforward inhibition, a process that may shape SPN spike timing, striatal processing and synaptic plasticity.

Key Words: methyllycaconitine; mecamylamine; DHβE; channelrhodopsin-2; striatal microcircuitry; tonically active neurons; paired-pulse ratio; postsynaptic potential; afterdepolarization

Introduction

As the main input nucleus of the basal ganglia, the striatum receives convergent cortical synaptic information, generating a computationally transformed interpretation of this information and relaying it to intermediate and output nuclei of the basal ganglia. Striatal output is carried exclusively by GABAergic striatal spiny projection neurons (SPNs), which account for ~95% of all striatal neurons (Gerfen and Surmeier 2011, Silberberg and Bolam 2015). The remaining 5% of striatal neurons are interneurons, most of which are GABAergic interneurons (GINs). There are several molecularly distinct classes of GINs that exhibit diverse intrinsic firing patterns and patterns of intrastriatal connectivity (Tepper, Tecuapetla et al. 2010, Muñoz-Manchado, Bengtsson Gonzales et al. 2018, Assous and Tepper 2019). In the context of feedforward cortico- and thalamo- striatal transmission the GINs' function lies in the feedforward inhibition they provide to SPNs (Tepper, Koós et al. 2004, Assous, Kaminer et al. 2017). Such inhibition can fashion striatal output by perturbing the precise timing of SPNs or prevent their spiking altogether. The only non-GABAergic interneurons are the large, aspiny, cholinergic interneurons (CINs) (DiFiglia 1987, Tepper and Bolam 2004, Plotkin and Goldberg 2019, Poppi, Ho-Nguyen et al. 2021). Despite their small numbers (approximately 1% of striatal neurons) the acetylcholine (ACh) they release influences the entire striatal microcircuitry. A single CIN axon can cover a third of the striatum (in linear dimension) and has ACh release sites every few micrometers (DiFiglia 1987). In fact, the striatum has the highest expression of cholinergic markers in the entire CNS (Mesulam, Mash et al. 1992, Contant, Umbriaco et al. 1996). CINs are autonomous pacemakers (Bennett and Wilson 1999) that are largely identified as the tonically active neurons (TANs) of the striatum (Kimura, Rajkowski et al. 1984, Wilson, Xu et al. 1990, Aosaki, Tsubokawa et al. 1994, Aosaki, Kimura et al. 1995, Morris, Arkadir et al. 2004), firing 3-10 spikes/s *in vivo*. On the backdrop of this ongoing discharge, the main signal they convey *in vivo* is a pause in response to primary reward or salient stimuli associated with reward (Aosaki, Tsubokawa et al. 1994, Morris, Arkadir et al. 2004, Goldberg and Reynolds 2011, Apicella 2017). The duration of the pause in response to a brief conditioned sensory stimulus is on the order of 200-300 ms (Kimura, Rajkowski et al. 1984, Raz, Feingold et al. 1996, Apicella, Legallet et al. 1997).

CINs regulate SPNs in 3 main ways. The best characterized regulation is exerted via muscarinic ACh receptors (mAChRs). Activation of presynaptic and postsynaptic mAChRs on SPNs modulates synaptic transmission, synaptic plasticity and the intrinsic excitability of SPNs by modulating various voltage-activated Ca^{2+} and K^{+} channels (Akins, Surmeier et al. 1990, Calabresi, Centonze et al. 1999, Gabel and Nisenbaum 1999, Day, Wokosin et al. 2008, Goldberg, Ding et al. 2012, Zucca, Zucca et al. 2018). CINs influence SPNs via nicotinic ACh receptors (nAChRs) as well, albeit indirectly. Activation of nAChRs on striatal dopaminergic fibers can evoke dopamine (DA) release (Zhou, Liang et al. 2001, Cachope, Mateo et al. 2012, Threlfell, Lalic et al. 2012, Liu, Cai et al. 2022) which, in turn, can modulate the intrinsic excitability of SPNs and synaptic transmission and plasticity at synaptic inputs. All of the above influences involve GPCR-linked ACh and DA receptors, which means that they are unlikely to dynamically affect the moment-by-moment processing and transmission of excitatory inputs to SPNs. Indeed, a recent study in which CINs were silenced optogenetically *in vivo* has put a lower bound on how fast mAChR-mediated effects can come into play. When CINs are synchronously silenced for over 500 ms, SPNs begin to show signs of mAChR-dependent reductions in excitability. However, that effect comes into play only after a 400 ms delay (Zucca, Zucca et al. 2018). The only known mechanisms by which CINs can rapidly affect SPN activity (sooner than 400 ms) involve nicotinic or muscarinic modulation of synaptic glutamate release or α4β2 nAChR-dependent GABA release onto the SPNs' ionotropic $GABA_A$ receptors (Pakhotin and Bracci 2007, English, Ibanez-Sandoval et al. 2011, Faust, Assous et al. 2015, Faust, Assous et al. 2016, Assous, Kaminer et al. 2017, Assous 2021). The α4β2 nAChRs that drive disynaptic GABA release are located on GINs (English, Ibanez-Sandoval et al. 2011, Faust, Assous et al. 2015), and on dopaminergic nigrostriatal terminals (Nelson, Hammack et al. 2014).

Because CINs receive massive excitatory cortical and thalamic input (Lapper and Bolam 1992, Thomas, Smith et al. 2000, Mamaligas, Barcomb et al. 2019) it is conceivable that their disynaptic inhibition of SPNs comes into play during bouts of

cortical or thalamic activity. However, this raises a conceptual problem. Because cortex and thalamus can activate feedforward inhibition to SPNs via various striatal GINs (e.g., cortex → GIN → SPN), what is gained by recruiting an additional pathway that is necessarily slower and less reliable due to its additional synapse (e.g., cortex → CIN → GIN → SPN)? Moreover, what is the role of nAChRs on GINs, such as the parvalbumin-positive fast-spiking interneurons (PV-FSIs) that only weakly respond to direct activation of CINs (English, Ibanez-Sandoval et al. 2011, Nelson, Bussert et al. 2014, Nelson, Hammack et al. 2014)? This conceptual problem exists only if we assume that the role of CINs in modulating SPN function through the activation of nAChRs is anchored around their phasic activation by excitatory afferents. In this study we demonstrate that ongoing CIN activity exerts a constant brake on SPN excitation and spike initiation via tonically activated α4β2 nAChRs located on discrete populations of GINs. We uncover these nicotinic effects using transgenic mice that nominally express channelrhodopsin-2 (ChR2) in corticostriatal fibers (Arenkiel, Peca et al. 2007). Activation of these fibers creates a competition between monosynaptic cortical excitation and polysynaptic feedforward inhibition to SPNs. We show that nAChRs embedded in a GABAergic post-synaptic pathway are capable of controlling SPN spike timing with millisecond precision.

Results

To interrogate microcircuit-level responses of SPNs to cortical excitation of the striatum, we generated acute *ex vivo* brain slices from Thy1-ChR2 mice, which nominally express ChR2 in cortical neurons (Arenkiel, Peca et al. 2007, Aceves Buendia, Tiroshi et al. 2019). Full-field optogenetic stimulation with a 470 nm LED engaged corticostriatal afferents and generated in SPNs either: excitatory postsynaptic potentials (EPSPs) for low LED intensities, or – in the suprathreshold condition – an action potential (AP) followed by an after depolarization (ADP) lasting 10s of milliseconds (Fig. 1a). While ADPs were kinetically similar to EPSPs under our experimental conditions, we explicitly separated these measures because ADPs 1) can be modulated by similar cortically-activated local striatal circuits that shape SPN spike timing and 2) peak closer to spike threshold, positioning them to influence subsequent spike generation (Flores-Barrera, Vizcarra-Chacón et al. 2010). Blockade of nAChRs with mecamylamine (mec; 10 μM)

enhanced SPN responses to cortical stimulation (Fig. 1b), as it shortened AP latency (Fig. 1c) and increased both the ADP (Fig. 1d) and subthreshold EPSP amplitudes (Fig. 1e). Because this suggests that under these conditions EPSPs and ADPs are mechanistically similar, the remainder of this study focuses on SPN AP latency and ADP amplitude generated by just-suprathreshold LED stimulation, that facilitated comparison among cells. The effects of mecamylamine were replicated in the presence of the α4β2 nAChR-selective antagonist, DHβE (10 μM, AP latency: n = 8 SPNs, p = $7.8 \cdot 10^{-3}$, SRT; ADP amplitude: n = 7 SPNs, p = 0.03, SRT; Fig. 1- figure supplement 1). Because the resting membrane potential of SPNs is very hyperpolarized compared to the depolarized potential from which spikes typically occur *in vivo* (Wilson and Groves 1981, Stern, Jaeger et al. 1998)], we repeated the experiment while holding the SPN with a constant positive current injection in the just-subthreshold region (e.g., in the –55 mV to –50 mV range). Mecamylamine shortened the latency to AP from this depolarized potential as well (Fig. 1f-g). We note that ADPs were not consistently present under these conditions, likely because the depolarized potential typically eclipsed ADP amplitudes observed from rest.

Because SPNs themselves do not express nAChRs, the action of mecamylamine must be indirect. Functional nAChR are expressed at multiple loci of the striatal circuit, including afferent axonal terminals and intrastriatal interneurons (Nelson, Hammack et al. 2014, Faust, Assous et al. 2016, Abudukeyoumu, Hernandez-Flores et al. 2019, Assous 2021, Abbondanza, Ribeiro Bas et al. 2022, Morgenstern, Isidro et al. 2022). While the broad antagonistic actions of mecamylamine and DHβE should block nicotinic receptors at most of these loci, α7 nAChRs, which are predominantly expressed at corticostriatal axon terminals, may be spared (Solinas, Scherma et al. 2007, Licheri, Lagström et al. 2018, Assous 2021). Indeed, mecamylamine did not have a significant effect on the strength or release probability of corticostriatal glutamatergic afferents, as measured by local electrical stimulation (Fig. 2a-c). Blockade of α7 nAChRs with the more selective α7 antagonist methyllycaconitine (MLA; 5 μM) did not significantly alter corticostriatal afferent strength or release probability either (Fig 2- figure supplement 1), suggesting that nAChRs on these synapses are not poised to track tonic ACh release.

The lack of an effect of mecamylamine on presynaptic release probability suggests that mecamylamine shapes SPN spike timing through postsynaptically expressed nicotinic receptors within the striatum. Cholinergic interneurons form a disynaptic circuit with SPNs, which is mediated by neuropeptide Y–neurogliaform (NPY-NGF) GINs (and perhaps other classes of nAChR-expressing GABAergic interneurons) in a nAChR-dependent manner (English, Ibanez-Sandoval et al. 2011, Elghaba, Vautrelle et al. 2016, Faust, Assous et al. 2016, Assous, Kaminer et al. 2017, Tepper, Koós et al. 2018). Consistent with the involvement of such an inhibitory polysynaptic circuit, we note that blockade of nAChRs reduced the latency of synaptically-evoked spikes in SPNs that were held just-subthreshold even if the SPN membrane potential fell (Fig. 1f), an observation that could be accounted for by GABA receptor mediated shunting (Gustafson, Gireesh-Dharmaraj et al. 2006). Accordingly, blockade of GABAergic transmission with the $GABA_A$ and $GABA_B$ receptor antagonists SR-95531 (10 μM) and CGP-55845 (2 μM), respectively, mimicked the effect of mecamylamine on spike timing and ADP amplitude (Fig. 3a-c). Blockade of GABA receptors fully occluded mecamylamine's effect on both spike latency and ADP amplitude (Fig. 3a-c), further implicating a CIN-GIN-SPN disynaptic circuit in mediating the actions of nAChRs. Strikingly, mecamylamine prevented GABA receptor antagonists from further advancing spike timing or enhancing ADP amplitude, suggesting that nAChR activation can saturate GABAergic inhibition (Fig. 3d-f).

While SPN spiking was driven by convergently activated corticostriatal inputs in the above experiments, activation of monosynaptic GABAergic inputs due to ectopic expression of ChR2 cannot necessarily be ruled out. This is an important point, because mecamylamine's mechanism of action involves nAChRs embedded in a GABAergic circuit. Immunohistochemical staining did not show any evidence of ChR2 expression in GABAergic neurons within the cortex or striatum, including somatostatin-expressing cortical neurons known to directly innervate SPNs (Rock, Zurita et al. 2016), but did reveal ChR2-positive neurons in the globus pallidus (Fig 3- figure supplement 1). This is in addition to observations of ChR2 expression in GABAergic neurons of the substantia

nigra pars reticulata in Thy1-ChR2 mice (Pan, Brown et al. 2013, Higgs and Wilson 2017, Tiroshi and Goldberg 2019). Indeed, blockade of glutamate receptors to eliminate feed forward inhibition revealed the presence of an optogenetically-evoked monosynaptic GABAergic input to SPNs (Fig 3- figure supplement). This monosynaptic input was insensitive to mecamylamine, however, making it unlikely to mediate the observed effect of nAChRs on SPN spike timing (Fig 3- figure supplement 1).

CINs receive converging excitatory inputs from the thalamus as well as the cortex (Lapper and Bolam 1992, Thomas, Smith et al. 2000). Indeed, targeted recordings from CINs confirmed that they are robustly engaged by our corticostriatal stimulation protocol, even displaying a lower stimulation threshold and shorter average delay to spike than SPNs (Fig. 4a-c). Despite the observed high fidelity and speed of cortically-evoked CIN spiking, a comparison of the temporal dynamics of synchronous cortical engagement of SPN inhibition (latency of approximately 5 ms, Fig. 5a) vs synchronous CIN engagement of GINs [latency of approximately 11 ms, (English, Ibanez-Sandoval et al. 2011, Nelson, Hammack et al. 2014)] shows that phasic activation of CINs is still not sufficiently fast to account for the mecamylamine-induced spike delay we observed in SPNs (Fig. 5b). In particular, even if there are sufficient numbers of CINs that respond *instantaneously* to cortical activation due to their ongoing activity, the earliest latency at which their phasic inhibition can influence SPNs is 11 ms later (English, Ibanez-Sandoval et al. 2011, Nelson, Hammack et al. 2014). However, SPN spikes are being delayed beginning 5 ms after stimulation (Fig. 5c magenta), which cannot be explained by phasic CIN activation.

If phasic activation of nAChRs by synaptically evoked CIN activity cannot account for the observed delay in SPN spike initiation (due to the necessarily slow nature of the CIN-GIN-SPN disynaptic signal), how does blocking nAChRs advance synaptically evoked SPN spiking? Given the autonomous pacemaking nature of CINs, perhaps the explanation is that *tonic*, rather than phasic, activation of nAChRs is key to the phenomenon. There are three obvious mechanisms that could be at play in this scenario: 1) ongoing nAChR activation (either tonic or phasic activation that is not time-

locked with the corticostriatal stimulation event leading to SPN spiking) may decrease SPN intrinsic excitability indirectly, likely by altering ongoing neuromodulator release (Zhou, Wilson et al. 2002, Rice and Cragg 2004) 2) the effect on SPN spiking may be a non-specific drug effect of mecamylamine (this is unlikely, since DHβE had the same effects) or 3) *tonic* activation of somatodendritic nAChRs may produce an ongoing depolarization of GINs, ultimately priming or accentuating corticostriatal feedforward inhibition.

To test the possibility that blockade of ongoing nAChR activation increases SPN excitability, we measured the current-voltage relationship of SPNs before and during mecamylamine application. While there is no indication that our detected effect of mecamylamine on spike timing or ADP amplitude is bimodal and specific to direct pathway SPNs (dSPNs) or indirect pathway SPNs (iSPNs), dSPNs and iSPNs display differences in basal excitability (Gertler, Chan et al. 2008), which can complicate interpretation. We therefore performed these experiments in transgenic mice where dSPNs and iSPNs could be identified by their fluorescent label (Shuen, Chen et al. 2008, Ade, Wan et al. 2011) (Fig. 6a). Mecamylamine had no significant effect on the resting membrane potential or rheobase current of either SPN type (Fig. 6b,c). Furthermore, mecamylamine did not decrease the time to spike in response to somatic rheobase current injection or the latency to first spike in an AP train induced by suprathreshold somatic current injection (Fig 6- figure supplement 1). Given that most data to this point came from pooled populations of SPNs, and that we observed no SPN-type specific effects of mecamylamine on SPN excitability, we performed additional analysis on pooled SPN data. While rheobase currents were unaffected, mecamylamine decreased the responsiveness to several sub-rheobase amplitude currents, arguing that if anything mecamylamine may *decrease* the excitability of SPNs in some regards (Fig. 6d). Mecamylamine had no effect on the firing rate of SPNs (Fig. 6e), nor did it alter IV properties of unidentified SPNs recorded from Thy1-ChR2 mice (Fig 6- figure supplement 1). Taken together, reduced spike latency induced by nAChR blockade cannot be explained by changes in SPN intrinsic excitability.

Because mecamylamine did not increase the intrinsic excitability of SPNs, we tested if nAChR blockade attenuated the basal inhibitory GABAergic influence that they are under. Indeed, mecamylamine significantly reduced the frequency of spontaneous inhibitory postsynaptic currents (sIPSCs) in a mixed population of SPNs (Fig. 7a-c). As SPNs lack nAChRs, the source of these attenuated sIPSCs is likely GINs. Indeed, various classes of GINs are excited, and their spontaneous activity is elevated, by tonic activation of nAChRs (Luo, Janssen et al. 2013, Muñoz-Manchado, Foldi et al. 2014, Ibáñez-Sandoval, Xenias et al. 2015, Elghaba, Vautrelle et al. 2016, Tepper, Koós et al. 2018). Because PV-FSIs express nAChRs and convey strong feedforward inhibition to SPNs (Koós and Tepper 1999, Tepper, Koós et al. 2004, Planert, Szydlowski et al. 2010), but only weakly respond to phasic activation of CINs (English, Ibanez-Sandoval et al. 2011), we made targeted current clamp recordings from PV-Cre x Ai9-tdTomato transgenic mice (Johansson and Silberberg 2020) and tested the effect of nAChR blockade on their excitability (Fig. 7d). Indeed, blocking nAChRs by bath application of DHβE significantly hyperpolarized the resting membrane potential of PV-FSIs (Fig. 7d-e)- this effect of nAChR blockade was not universally observed in other populations of GINs that are involved in feed forward inhibition, such as spontaneously firing somatostatin (SOM)+ interneurons, in which mecamylamine had no effect on firing rate and actually depolarized the average membrane potential (Fig 7- figure supplement 1). Thus, tonic activation of nAChRs depolarizes the resting membrane potential of PV-FSIs, continuously holding them closer to the AP threshold, and thereby priming them to transmit cortically-driven feedforward inhibition more efficiently to SPNs. Interestingly, the dependence upon trailing “primed” GIN input may explain why mecamylamine was capable of diminishing the amplitude of relatively slow rising EPSPs (Fig. 1e) but not faster peaking EPSCs (Fig. 2b).

If SPN spike latency is perpetually slowed due to tonic nAChR-mediated “priming” of presynaptic GINs, then taking the relevant GINs offline should mimic and occlude the effect of mecamylamine. Unlike some other GINs that target SPNs, such as persistent/plateau-low-threshold spiking (LTS) interneurons (Tepper, Tecuapetla et al. 2010, Plotkin and Goldberg 2019), synaptic responses of PV-FSIs to cortical inputs are

mediated by Ca^{2+}-permeable AMPA receptors that lack the GluA2 subunit (Gittis, Nelson et al. 2010). In fact, pharmacological blockade of Ca^{2+}-permeable GluA2-lacking AMPA receptor subunits prevents cortical activation of PV-FSIs but not persistent/plateau-LTS interneurons (Gittis, Nelson et al. 2010, Gittis, Leventhal et al. 2011). Indeed, pharmacologically preventing cortical activation of PV-FSIs with the Ca^{2+}-permeable AMPA receptor antagonist 1-Naphthyl acetyl spermine (Naspm; 100 μM) not only reduced spike latency and ADP amplitude, but occluded the effect of mecamylamine (Fig. 8). Taken together, these data demonstrate that tonic activation of nAChRs on a subclass of GINs is responsible for delaying cortically-evoked SPN spiking, and implicate PV-FSIs as the primary mediator.

In summary, the tonic activity of CINs recruits a subclass of GINs, namely PV-FSIs, to provide a “nicotinic brake” on SPN responsiveness to cortical activity (Fig. 9). Such a mechanism could allow SPNs to be more receptive of cortical inputs when CINs pause their firing in response to salient inputs or stimuli associated with reward.

Discussion

The present study describes a novel role for tonic nAChR activation in shaping striatal output. Decades of research have firmly established CINs as important modulators – mostly via muscarinic ACh receptors (Goldberg, Ding et al. 2012, Zucca, Zucca et al. 2018, Assous 2021) – of cortico- and thalamo- striatal synaptic integration and determinants of striatal output (Akins, Surmeier et al. 1990, English, Ibanez-Sandoval et al. 2011, Abudukeyoumu, Hernandez-Flores et al. 2019). Despite the fact that CINs are autonomous pacemakers, nearly all studies examining their influence on the precise temporal output of the striatum, particularly via nAChRs, have been centered around the consequences of their phasic engagement (Witten, Lin et al. 2010, English, Ibanez-Sandoval et al. 2011, Faust, Assous et al. 2016, Dorst, Tokarska et al. 2020). Here we report that ongoing, non-phasic activation of nAChRs accounts for a basal elevation in GABAergic tone, which dampens the response of SPNs to convergent cortical inputs and ultimately delays striatal output.

Basal cholinergic regulation of striatal output- a postsynaptic "nicotinic brake"?
CINs can robustly evoke GABAergic inhibition in the striatum by engaging somatodendritic nAChRs on specific classes of local GINs, in particular those expressing NPY (English, Ibanez-Sandoval et al. 2011, Luo, Janssen et al. 2013). This cell-type specific nAChR-dependent mechanism has been demonstrated using electrical or optogenetic stimulation to drive *phasic,* stimulation-locked inhibition. Somewhat puzzling, however, are reports that certain GINs, including PV-FSIs, only weakly respond to phasic activation of CINs [or cholinergic afferents from the midbrain (Dautan, Huerta-Ocampo et al. 2020)] even though they express the requisite somatodendritic nAChRs (Koós and Tepper 2002, English, Ibanez-Sandoval et al. 2011, Nelson, Bussert et al. 2014, Nelson, Hammack et al. 2014). Our finding that tonic activation of nAChRs enhances the excitability of FSIs, as has been shown previously (Koós and Tepper 2002, Luo, Janssen et al. 2013), offers a physiological role for these receptors. In fact, tonic activation of nAChRs on FSIs (driven by the tonic activity of CINs) may partly explain why previous studies have only observed modest responses of FSIs to additional phasic stimulation of CINs (English, Ibanez-Sandoval et al. 2011, Nelson, Bussert et al. 2014).

Tonic nAChR excitation of GINs helps clarify another puzzling observation. It is obvious why GABAR blockers occlude the effect of mecamylamine on AP latency and ADP amplitude in SPNs- the relevant GABARs are synaptically downstream of the nAChRs on GINs. But why is it that mecamylamine seems to "saturate" the effect of GABAR inhibition on SPN AP latency and ADP? In other words, why does blockade of GABARs have no additional effect on AP latency or ADP when applied after mecamylamine, when phasic CIN activation only engages a select few types of GINs? If nAChRs were recruited solely by phasic activation of CINs, then the addition of GABAR blockers after mecamylamine should further shorten the AP latency and increase ADP amplitude by attenuating the influence of other GINs (such as PV-FSIs) that are only weakly responsive to phasic activation of nAChRs (English, Ibanez-Sandoval et al. 2011, Nelson, Bussert et al. 2014, Nelson, Hammack et al. 2014). A "priming" effect of tonic

nAChR activation on GINs that are not directly driven to spike by CINs could explain the seemingly oversized influence of nicotinic signaling on GABAergic inhibition.

While an exhaustive categorization of the role every GIN class plays (or doesn't play) in mediating the observed effect may be ill-posed, we have identified PV-FSIs as the likely primary contributor. First, blockade of nAChRs hyperpolarized PV-FSIs at rest, suggesting that tonic activation of nAChRs holds these GINs closer to spike threshold. We observed the opposite effect in a similar class of GINs that mediates feedforward inhibition (SOM+ interneurons), making their involvement in the process less likely. While the effect on PV-FSI resting membrane potential that we observed was modest, we note that a similar magnitude mecamylamine-induced hyperpolarization is sufficient to slow the spontaneous firing rate of NPY-expressing LTS interneurons (Elghaba, Vautrelle et al. 2016). Second, pharmacologically blocking cortical activation of PV-FSIs with a Ca^{2+}-permeable AMPA receptor antagonist, which leaves synaptic activation of other GINs such as persistent/plateau-LTS interneurons intact, completely occluded the effect of mecamylamine on SPN spike latency. Together, these data corroborate PV-FSIs as the primary candidate to exert the 'nicotinic brake' we observed during basal circuit activity.

Under what conditions will the 'nicotinic brake' be lifted?

Through their continuous autonomous discharge, CINs tonically-release ACh in the striatum (Zhou, Wilson et al. 2002). While a prolonged exposure of striatal nAChRs to ACh is bound to desensitize them, it has been argued that the fast action of striatal acetylcholinesterase (AChE) prevents nAChR desensitization, allowing for the maintenance of tonic nAChR activation in the striatum (Zhou, Wilson et al. 2002). So if tonic nAChR activation normally puts a brake on cortical feedforward inhibition, under what circumstances is this brake removed? The tonically active neurons (TANs) of the primate striatum, which are comprised mainly of CINs (Wilson, Xu et al. 1990, Aosaki, Kimura et al. 1995), acquire a synchronized pause response (Raz, Feingold et al. 1996) in their tonic firing that lasts several hundred milliseconds in response to primary reward or, through conditioning, to salient stimuli associated with reward (Kimura, Rajkowski et

al. 1984, Apicella, Legallet et al. 1997, Goldberg and Reynolds 2011, Bradfield, Bertran-Gonzalez et al. 2013). This pause duration should be sufficient – particularly while AChE rapidly clears the extracellular space from ACh – to deactivate the nAChRs, thereby removing the nicotinic brake.

Our study complements a recent study that described how CINs impact SPN neural dynamics *in vivo* (Zucca, Zucca et al. 2018). In that study it was shown that when CINs are optogenetically silenced in a synchronous-fashion for a sufficiently long period SPNs become hyperpolarized, less excitable and short-term corticostriatal plasticity is dampened. However, these effects commence only 400 ms after CINs are silenced. Until that point SPN excitability is unaffected. Thus, that study remained agnostic about the effect of CIN pauses that are shorter than 400 ms long on SPNs. Because physiological TAN pauses in response to sensory cues are typically over after 300 ms (Kimura, Rajkowski et al. 1984, Apicella, Legallet et al. 1997), the mAChR-mediated curbing of SPN excitability and responsiveness revealed in that and other studies (Ebihara, Yamamoto et al. 2013) may not be relevant to the role of the shorter, more physiological CIN pauses. Assuming that the nAChR-dependent mechanism we revealed can come into play sooner, our findings suggest that there are two dichotomous phases to the effect of synchronous CIN pauses: an 'early' period that is dominated by the consequences of removing tonic nAChR activation, and a more delayed period driven by diminished activation of mAChRs, where the responsiveness of SPNs to incoming cortical input is weakened, as shown previously (Zucca, Zucca et al. 2018).

Implications for tuning striatal circuit activity

Our data suggest that as CIN pauses develop ongoing GABAergic inhibition will be relieved. This could have the effect of sharpening the timing of cortically-driven spiking by several milliseconds, ultimately shaping the moment-by-moment processing of striatal output. Because the TAN pause usually coincides with the arrival of a salient stimulus, it is precisely a moment when SPNs need to be more attuned to cortical input and respond more reliably. Given the relatively higher affinity of α4β2 vs α7 nAChRs

(Albuquerque, Pereira et al. 2009) it is not surprising that we found α7-mediated boosting of presynaptic glutamate release to be insensitive to tonic ACh levels, setting the stage for a CIN pause-initiated drop in ACh levels to promote a temporal sharpening of any proceeding SPN spikes that are induced. Moreover, seminal experiments in primates have shown that CIN pauses become more prominently and reliably evoked by sensory stimuli over the course of Pavlovian conditioning (Aosaki, Tsubokawa et al. 1994, Aosaki, Kimura et al. 1995). Together, this implies that removal of the 'nicotinic brake' may be a crucial component of striatal learning. While a several milliseconds shift in spike timing may not seem like much in the context of 100s of milliseconds long CIN pauses or SPN state transitions, it may be ample time to move a spike into or out of the time window for NMDA receptor-dependent coincidence detection to occur (Hao and Oertner 2012).

Both dSPNs and iSPNs robustly support spike timing dependent plasticity (STDP) (Pawlak and Kerr 2008, Shen, Flajolet et al. 2008). Under permissive conditions, constraining the relative timing of SPN APs to occur 5 milliseconds after a corticostriatal synaptic burst efficiently potentiates the active synapses (Shen, Flajolet et al. 2008). In this view, decreasing the time to spike on the time scale we observe may be sufficient to bring the spike temporally close enough to NMDA receptor activation to engage the signaling cascades that are crucial for long term potentiation. Such subtle nAChR-dependent tuning could be a way of 'distancing' those same cortical afferents from SPN activity under conditions of basal activity, allowing for the synapses encoding a particular sensorimotor cue to become potentiated only when deemed appropriate by a learned cholinergic signal. Expanding upon this possibility, it was recently shown that synapse-specific corticostriatal long term potentiation requires the coordination of CIN pauses with dopamine release and SPN depolarization (Reynolds, Avvisati et al. 2022). It is tempting to speculate that a function of the CIN pause in the scenario is to create a window of plasticity by removing the 'nicotinic brake' to reduce synaptic inhibition and promote and adjust the latency of evoked spikes.

The extent to which tonic activation of nAChRs will be capable of influencing GABA release and SPN responses to cortical inputs will likely depend on the capacity of AChE activity to both allow for the detection of a CIN pause, and minimize nAChR desensitization (Zhou, Wilson et al. 2002). This brings up an important corollary of the 'nicotinic brake' hypothesis: the putative mechanism by which CIN pauses remove the nicotinic brake may be most robust in the AChE-enriched compartment of the striatum, also known as the matrix (as opposed to striosomes) (Graybiel and Ragsdale 1978, Brimblecombe and Cragg 2017, Prager and Plotkin 2019). Because the matrix constitutes ~85% of the striatum, our data likely reflect the situation in that compartment (Prager and Plotkin 2019). While coordinated CIN activation can interrupt the timing of ongoing APs in both matrix and striosome SPNs (Crittenden, Lacey et al. 2017), the degree of tonic nAChR activation and existence of a 'nicotinic brake' in striosomes is unclear.

Taken together, our data suggest an additional role for cholinergic signaling in shaping striatal activity. While a great deal is known about how ACh can impact SPN function through metabotropic muscarinic receptors, nearly all studies of the 'faster' nAChR arm of ACh signaling have focused on its phasic activation. The data in this study demonstrate that nAChR signaling is not constrained to times of phasic CIN engagement, and tonic activation of nAChRs places a 'brake' on SPN activity that may help guide the fine tuning of striatal output.

Materials and Methods

Key Resources Table				
Reagent type (species) or resource	**Designation**	**Source or reference**	**Identifiers**	**Additional information**
Genetic reagent (*M. musculus*)	C57BL/6J	Jackson Laboratory	RRID: IMSR_JAX:000664	
Genetic reagent (*M. musculus*)	B6.FVB-Tg(Drd2-EGFP/Rpl10a)CP101Htz/J	Jackson Laboratory	RRID: IMSR_JAX:030255	
Genetic reagent (*M. musculus*)	B6.Cg-Tg(Drd1-tdTomato)6Calak/J	Jackson Laboratory	RRID: IMSR_JAX:016204	
Genetic reagent (M. musculus)	B6.Cg-Tg(Thy1-COP4/EYFP)18Gfng/J	Jackson Laboratory	RRID:IMSR_JAX:007612	
Genetic reagent (*M. musculus*)	PV-cre	Jackson Laboratory	RRID: IMSR_JAX:017320	
Genetic reagent (*M. musculus*)	Som-cre	Jackson Laboratory	RRID: IMSR_JAX:018973	
Genetic reagent (*M. musculus*)	Ai9 (‘tdTomato’)	Jackson Laboratory	RRID: IMSR_JAX:007909	

Virus	AAV5-Ef1a-DIO-EYFP	addgene	27056-AAV5	
Chemical compound, drug	Mecamylamine hydrochloride	Sigma-Aldrich Tocris	Lot # 019M4108V CAS: 826-39-1 #2843, CAS: 110691-49-1	
Chemical compound, drug	Dihydro-β-erythroidine hydrobromide	Tocris	#2349, CAS: 29734-68-7	
Chemical compound, drug	SR 95531 hydrobromide (Gabazine)	Hello Bio	CAS: 104104-50-9	
Chemical compound, drug	DNQX	TOCRIS	CAS: 2379-57-9	
Chemical compound, drug	D-AP5	Hello Bio	CAS:79055-68-8	
Chemical compound, drug	Methyllycaconitine citrate	TOCRIS	Lot # 23A/255947 CAS:351344-10-0	
Chemical compound, drug	Naspm trihydrochloride	Alomone Labs	CAS: 1049731-36-3	
Chemical compound, drug	CGP 55845 hydrochloride	Hello Bio	CAS: 149184-22-5	

Chemical compound, drug	XYLAZINE AS HYDROCHLORIDE	EUROVET ANIMAL HEALTH B.V	CAS: 082-91-92341-00	
Chemical compound, drug	CLORKETAM	VETOQUINOL	CAS: 1867-66-9	
Chemical compound, drug	VECTASHIELD® Vibrance™ Antifade Mounting Medium with DAPI	VECTOR LABORATORIES	SKU: H-1800	
Antibody	Recombinant Anti-GAD65 + GAD67 antibody [EPR19366]	abcam	ab183999	
Antibody	Rabbit polyclonal anti Somatostatin-14	Peninsula Laboratories	T-4102	

Animals

All experimental procedures on mice adhered to and received prior written approval from the Institutional Animal Care and Use Committees of the Hebrew University of Jerusalem and of Stony Brook University and of the local ethics committee of Stockholm, Stockholms Norra djurförsöksetiska nämnd. Experiments were conducted on various transgenic mice. For optogenetic activation of corticostriatal fibers, we used 1-4 months old male and female homozygous transgenic Thy1-ChR2 mice [B6.Cg-Tg(Thy1-COP4/EYFP)18Gfng/J] that express channelrhodopsin-2 under the Thy1 promoter were used. Thy1-ChR2 mice express ChR2 in cortical afferents under the thymus cell antigen 1 (Thy1) promoter. Thy1 is generally expressed in the axons of

layer V pyramidal neurons, limbic system, midbrain and brainstem (Arenkiel, Peca et al. 2007) . For experiments measuring paired pulse ratios (PPRs), neuronal excitability and spontaneous GABAergic events, we used 1.5-4 month old male and female C57bl/6 mice crossed with one of two BAC transgenic lines (where indicated): drd1-tdTomato (labeling dSPNs) or drd2-eGFP (labeling iSPNs) (Shuen, Chen et al. 2008, Ade, Wan et al. 2011). For PV-FSI and SOM+ interneuron recordings, both male and female mice (postnatal days 47-82) were used in this study. Mice were group-housed under a 12 hr light / dark schedule and given ad libidum access to food and water. The PV-Cre (stock #017320, the Jackson laboratory) mouse line was crossed with a homozygous tdTomato reporter mouse line ('Ai9', stock #007909, the Jackson laboratory) to allow identification of FSIs based on the expression of a fluorescent marker protein. SOM+ interneurons were identified by injecting cre-dependent AAV (27056-AAV5, addgene) into the striatum of SOM-cre mice, inducing the expression of YFP in SOM-positive neurons specifically (stock #018973, the Jackson Laboratory). The PV- and SOM- Cre lines were heterozygous and maintained on a wild-type C57BL/6J background (stock # 000664, the Jackson Laboratory).

Virus injections

Som-cre mice were anesthetized with isoflurane and placed in a stereotaxic frame (Havard Appartus, Holliston, MA). A Quintessential Stereotaxic Injector (Stoelting, Wood Dale, IL) was used to inject 0.5 ul of AAV5-EF1a-DIO-EYFP (#27056, addgene) into the striatum (+0.5 AP, 2 ML, 2.5 DV) at a speed of 0.1 ul / minute. The pipette was held in place for at least 5 min after the injection. Following the surgery, the mice were given analgesics (Buprenorphine, 0.08 mg/kg, i.p.).

Slice preparation

For optogenetic activation experiments, PPR, excitability and spontaneous GABAergic event experiments: Mice were deeply anesthetized with ketamine–xylazine and perfused transcardially with ice-cold modified artificial cerebrospinal fluid (ACSF) bubbled with 95% O_2–5% CO_2, and containing (in mM): 2.5 KCl, 26 $NaHCO_3$, 1.25 Na_2HPO_4, 0.5 $CaCl_2$, 10 $MgSO_4$, 0.4 ascorbic acid, 10 glucose, and 210 sucrose

(optogenetic activation studies) or 3 KCl, 26 $NaHCO_3$, 1 NaH_2PO_4, 1 $CaCl_2$, 1.5 $MgCl_2$, 124 NaCl and 14 glucose (PPR, excitability and spontaneous GABAergic event measures). The brain was removed and sagittal or coronal slices (sectioned at a thickness of 275 µm were obtained in ice-cold modified ACSF. Slices were then submerged in ACSF, bubbled with 95% O_2–5% CO_2, and containing (in mM): 2.5 KCl, 126 NaCl, 26 $NaHCO_3$, 1.25 Na_2HPO_4, 2 $CaCl_2$, 2 $MgSO_4$, and 10 glucose and stored at room temperature for at least 1 h prior to recording (optogenetic activation studies), or 3 KCl, 26 $NaHCO_3$, 1 NaH_2PO_4, 2 $CaCl_2$, 1 $MgCl_2$, 124 NaCl and 14 glucose, incubated at 32°C for 45 then held at room temperature until recording (PPR, excitability and spontaneous GABAergic event measures).

For PV-FSI and SOM+ experiments: Mice were deeply anaesthetized with isoflurane and decapitated. The brain was removed and immersed in ice-cold cutting solution containing 205 mM sucrose, 10 mM glucose, 25 mM NaHCO3, 2.5 mM KCl, 1.25 mM NaH2PO4, 0.5 mM CaCl2 and 7.5 mM MgCl2. Parasagittal brain slices (thickness 250 mm) were prepared with a Leica VT 1000S vibratome and incubated for 30 – 60 min at 34˚C in a submerged chamber filled with artificial cerebrospinal fluid (ACSF) saturated with 95% oxygen and 5% carbon dioxide. ACSF was composed of 125 mM NaCl, 25 mM glucose, 25 mM NaHCO3, 2.5 mM KCl, 2 mM CaCl2, 1.25 mM NaH2PO4, 1 mM MgCl2. Subsequently, slices were kept for at least 30 min at room temperature before recording.

Slice visualization, electrophysiology and optogenetic stimulation

For optogenetic activation experiments: The slices were transferred to the recording chamber mounted on an Olympus BX51 upright, fixed-stage microscope and perfused with oxygenated ACSF at room temperature. A 60X, 0.9 NA water-immersion objective was used to examine the slice using Dodt contrast video microscopy. Patch pipette resistance was typically 3-4 MΩ when filled with recording solutions. In voltage-clamp experiments of IPSCs in SPNs the intracellular solution contained (in mM): 127.5 $CsCH_3SO_3$, 7.5 CsCl, 10 HEPES, 10 TEA-Cl, 4 phosphocreatine disodium, 0.2 EGTA, 0.21 Na_2GTP, and 2 $Mg_{1.5}ATP$ (pH=7.3 with CsOH, 280-290 mOsm/kg). For whole-cell current clamp recordings from SPNs and cell-attached recordings from CINs the pipette

contained (in mM): 135.5 KCH_3SO_4, 5 KCl, 2.5 NaCl, 5 Na-phosphocreatine, 10 HEPES, 0.2 EGTA, 0.21 Na_2GTP, and 2 $Mg_{1.5}ATP$ (pH=7.3 with KOH, 280-290 mOsm/kg). Electrophysiological recordings were obtained with a Multiclamp 700B amplifier (Molecular Devices, Sunnyvale, CA). Junction potential, which was 7-8 mV, was not corrected. Signals were digitized at 10 kHz and logged onto a personal computer with the Winfluor software (John Dempster, University of Strathclyde, UK). Blue light LED (470 nm, Mightex, Toronto, Ontario, Canada) was used for full-field illumination via the objective. Single pulses were 1 ms long. In order to compare action potential (AP) latency and afterdepolarization (ADP) amplitude among SPNs the LED intensity was set to generate a just suprathreshold response in each SPN recorded.

For PPR, excitability and spontaneous GABAergic event experiments: The slices were transferred to the recording chamber mounted on a modified Ultima laser scanning microscope system (Bruker Nano) (excitability and spontaneous GABAergic event experiments) or an Olympus BX51W1 microscope (PPR experiments) and perfused with oxygenated ACSF at room temperature. A 60X, 1.0 NA Olympus LUMPFL water-immersion objective was used to visualize slices, and fluorescently labeled neurons identified for recordings with the aid of a Dodt contrast image displayed in registration with the fluorescence image for experiments requiring identification of dSPNs vs iSPNs. Patch pipette resistance was typically 3-6 MΩ when filled with recording solutions. For voltage-clamp recordings the intracellular solution contained (in mM): 120 $CsMeSO_3$, 5 NaCl, 10 TEA-Cl (tetraethylammonium-Cl), 10 HEPES, 5 Qx-314, 4 ATP-Mg^{2+}, 0.3 GTP-Na^+, 0.25 EGTA, and 0.05 Alexa Fluor 568 hydrazide Na^+salt (Alexa Fluor was omitted in PPR experiments). For current clamp recordings the internal solution contained (in mM): 135 $KMeSO_4$, 5 KCl, 10 HEPES, 2 ATP-Mg^{2+}, 0.5 GTP-Na^+, 5 phosphocreatine-tris, 5 phosphocreatine-Na^+, 0.1 Fluo-4 pentapotassium salt, and 0.05 Alexa Fluor 568 hydrazide Na^+ salt. Patched SPNs were allowed to equilibrate for 10 min after rupture. Recordings were made using a Multiclamp 700B amplifier and either PrairieView 5.0 software (Bruker) or custom MATLAB protocols. sIPSCs were recorded in voltage-clamp mode at +10 mV for 180 seconds before and after bath application of drug. Access resistance and holding current were monitored throughout experiments and cells were excluded if these values changed by more than 20%. Local electrical

stimulation was evoked using a concentric bipolar stimulation electrode (FHC, Inc., Bowdoin, ME) placed near the cell using a stimulating amplitude of ~1-3 mV and 50 ms between stimuli pulses; 10 sweeps (10 s inter-sweep interval) were averaged per cell; cells were held at -70mV. PPR experiments were performed at 26-29°C. Rheobase & action potential firing frequencies were determined in current-clamp mode via a step series of 500 ms current injections starting at -200 pA and increasing by 25 pA with each step. Resting membrane potential & cell morphology were monitored throughout experiments and cells were excluded if resting at a more depolarized potential than -77.0 mV.

For PV-FSI and SOM+ experiments: Whole-cell patch clamp recordings were obtained in oxygenated ACSF at 35˚C. Neurons were visualized using infrared differential interference contrast (IR-DIC) microscopy (Zeiss FS Axioskop, Oberkochen, Germany). tdTomato- or EYFP- expressing neurons were identified by switching to epifluorescence using a mercury lamp (X-cite, 120Q, Lumen Dynamics). Borosilicate pipettes of 5 – 8 MOhm resistance were pulled with a Flaming / Brown micropipette puller P-1000 (Sutter instruments). All recordings were done in current clamp with an intracellular solution containing 130 mM K-gluconate, 5 mM KCl, 10 mM HEPES, 4 mM Mg-ATP, 0.3 mM GTP, 10 mM Na2-phospho- creatine (pH 7.25, osmolarity 285 mOsm). Recordings were amplified using a MultiClamp 700B amplifier (Molecular Devices, CA, USA), filtered at 2 kHz, digitized at 10-20 kHz using ITC-18 (HEKA Elektronik, Instrutech, NY, USA), and acquired using custom-made routines running on Igor Pro (Wavemetrics, OR, USA). Liquid junction potential was not corrected. Throughout all recordings pipette capacitance and access resistance were compensated for and data were discarded when access resistance increased beyond 30 MOhm. The intrinsic properties of the neurons were determined by a series of hyperpolarizing and depolarizing current steps and ramps, enabling the extraction of sub- and suprathreshold properties. All neurons were recorded in control conditions and after >5 min of bath application of 1 μM DHβE (Tocris) or 10 μM Mec (Tocris).

Drugs and Reagents

Experiments in Thy1-ChR2 mice were performed in the presence or absence of synaptic receptor blockers including 10 μM SR-95531 (gabazine) to block $GABA_A$ receptors, 2 μM CGP-55845 to block $GABA_B$ receptors, 10 μM mecamylamine, a non-selective nAChR-antagonist, 1 or 10 μM Dihydro-β-erythroidine hydrobromide (DHβE), a competitive α4β2 nAChR antagonist and Naspm (100 μM), a Ca^{2+}-permeable AMPA receptor antagonist. Experiments were conducted with various combinations of the blockers. The acute effects of solution exchanges were measured at least 5 min after wash on. All drugs and reagents were acquired from Tocris (Ellisville, MO, USA), Sigma (St. Louis, MO) or HelloBio (Bristol, Avonmouth, UK).

Histology

Nine week old female mice were deeply anesthetized with ketamine-xylazine followed by cold perfusion to the heart of PBS and 4% PFA. The removed brain was kept overnight at 4°C in 4% 4% PFA. The next day, the brain was washed in PBS (3 times, 20 min each) before thin 40μm coronal slices were made using a vibratome (LIECA VT1000 S). Slices were briefly washed with CAS-BLOCK (Life Technologies) before being incubated in CAS-BLOCK (300uL) overnight with GAD65+67 antibodies (ab183999 Abcam, 1:1000) or Somatostatin (BMA biomedicals Peninsula Laboratories T-4102, 1:100). The slices were then washed in PBS (3 times, 20 min each) and incubated with CAS-BLOCK and secondary antibodies (Abcam ab150063, 1:500) for 3 hours. Antifade Mounting Medium (VECTASHIELD) was applied to prevent slice bleaching.

Data Analysis and Statistics

Data analysis was performed using custom-made code in MATLAB (MathWorks, Natick, MA, USA) or Python; sIPSCs were analyzed using the Mini Analysis program (Synaptosoft). Two-tailed Wilcoxon signed-rank test (SRT) was used to test for changes of medians in matched-paired comparisons. The null hypotheses were rejected if the P values were below 0.05. Boxplots represent range (whiskers), median (thick bar) and lower and upper quartiles. To analyze responses to stimulation, peristimulus time histograms (PSTH) were generated. PSTH were estimated using 20 ms wide bins. IV

relationships, sIPSC frequencies and inter-event intervals were analyzed by two-way ANOVA.

Funding: BSF grant 2017020 to JLP and JAG. ISF grant 154/14 to JAG. ERC Consolidator (646880) to JAG. R01 NS104089/NINDS and NS022061/NINDS to JLP. Swedish Brain Fund (Hjärnfonden) grant to GS (FO2021-0333) and YJ (PS2020-0020). Swedish Research Council (VR-M) grant to GS (2019-01254). GS is supported by a Wallenberg Academy Fellowship (KAW 2017.0273).

Figure Captions

Fig. 1. nAChR-dependent inhibition and delay of spike latency in spiny projection neurons (SPNs) activated by corticostriatal fibers. A. Left: diagram of recording configuration. An SPN is patched in an acute slice from a Thy1-ChR2 mouse. Right: 1-ms-long 470 nm LED pulse of increasing intensity generates excitatory postsynaptic potentials (EPSPs), or an AP followed by an after depolarization (ADP) in an SPN. **B.** Examples of the effect of 10 μM mecamylamine (mec), an nAChR antagonist, on EPSP amplitude (dashed) or spike latency and ADP amplitude (solid). **C-E.** Mecamylamine significantly shortens spike latencies ($p = 4.8 \cdot 10^{-4}$, n = 12 SPNs, SRT) (**C**), as well as ADP ($p = 2.4 \cdot 10^{-3}$, n = 12 SPNs, SRT) (**D**) and EPSP ($p = 0.03$, n = 6 SPNs, SRT) (**E**) amplitudes. **F**. Examples of the effect of mecamylamine on latency of a spike triggered synaptically from a depolarized potential with an LED pulse. **G**. Mecamylamine significantly shortens spike latencies in SPNs held at a depolarized potential ($p = 0.03$, n = 6 SPNs, SRT). Two-sided Wilcoxon Signed-Rank test (SRT). *** $p < 0.001$, ** $p < 0.01$, * $p < 0.05$.

Fig. 2. Mecamylamine does not alter release probablity of excitatory synaptic inputs. A. Example responses of an SPN to paired pulse stimulation (evoked by two local electrical stimuli separated by 50 ms), before and in the presence of mecamylamine (10 μM). **B.** Mecamylamine had no effect on the EPSC amplitude evoked by the first paired stimulus (P1) ($p = 0.59$, n = 15 SPNs, SRT). **C.**

Mecamylamine had no effect on the paired pulse ratio (PPR) (P2/P1, $p = 0.33$, n = 15 SPNs, SRT).

Fig. 3. The nAChR-dependent inhibition of corticostriatal SPN activation is mediated through and saturates GABAergic inhibition. A. Example of the occlusion of the mecamylamine effect on optogenetic synaptic activation of SPNs by receptor (GABAR) antagonists, 10 μM SR-95531 ($GABA_AR$ antagonist) and 2 μM CGP-55845 ($GABA_BR$ antagonist). Distribution of spike latencies (**B**) and ADP amplitude (**C**) in response to application of GABAR antagonists followed by mecamylamine, show that application of GABAR antagonist significantly shortens the AP latency ($p = 4.6 \cdot 10^{-3}$, n = 13 SPNs, SRT) and enhancement of the ADP amplitude ($p = 2.4 \cdot 10^{-4}$, n = 13 SPNs, SRT). In contrast, the subsequent mecamylamine application fails to further shorten the AP latency ($p = 0.0625$, n = 5 SPNs, SRT) or further enhance the ADP amplitude ($p = 1$, n = 5, SRT). **D.** Example of how the mecamylamine effect saturates the GABAergic inhibition of the optogenetic synaptic activation of SPNs. **E-F.** Distribution of spike latencies (**E**) and ADP amplitude (**F**) in response to application of mecamylamine followed by GABAR antagonists, showed that the subsequent application of GABAR antagonists fails to further shorten the AP latency ($p = 0.25$, n = 5 SPNs, SRT) or further enhance the ADP amplitude ($p = 0.44$, n = 5 SPNs, SRT).

Fig. 4. The autonomous firing of cholinergic interneurons (CINs) enables them to respond more rapidly and vigorously than SPNs to feedforward corticostriatal excitation. A. Example of the autonomous discharge of a CIN recorded in cell-attached configuration (top) and the distribution of firing rates (bottom, n = 15 CINs) in an acute striatal slice. **B**. Peristimulus histograms (PSTHs) of a CIN in response to optogenetic activation of corticostriatal fibers at various 470 nm LED intensities as compared to the amplitude of the EPSPs evoked in a nearby SPN (insets), demonstrates that CINs are much more sensitive than SPNs to cortical activation. **C**. Cumulative distribution of the latency to first spike of CINs recorded in cell-attached mode (green, n = 8 CINs) as compared to the latency to first spike in an SPN recorded (from a resting-state) in the

whole-cell mode (n = 12), before (black) and after (magenta) application of mecamylamine.

Fig. 5. Latency of feedforward GABAergic IPSCs in SPNs activated synaptically by corticostriatal fibers. A. Left: IPSCs recorded in an SPN held at +10 mV before (black) and after (red) application of GABAR antagonists, reveals GABA-sensitive (purple) IPSC. Right: Zoom in of the GABAergic IPSCs enables estimation (fit of diagonal black line) of the latency of the feed-forward GABA-sensitive inhibition. **B.** Distribution of the latency of feedforward GABAergic inhibition to SPNs in the Thy1-ChR2 mouse (n = 7 SPNs). **C**. Schematic demonstrating that the feedforward GABAergic inhibition precedes the earliest timing of feedforward cholinergic di-synaptic inhibition of SPNs, indicating that phasic activation of CINs cannot explain the nAChR-dependent delay of spike latency.

Fig 6. SPN intrinsic excitability is not increased by nAChR-blockade. A. Example IV traces of dSPNs and iSPNs in the absence and presence of 10 μM mecamylamine. **B.** Left: resting membrane potential of dSPNs (black) and iSPNs (blue) in the absence and presence of mecamylamine (all SPNs: $p = 0.43$, n = 13; dSPNs: $p = 0.16$, n = 7; iSPNs: $p = 0.87$, n = 6; SRT). Right: percent change in resting membrane potential after mecamylamine application. **C.** Left: rheobase current of dSPNs and iSPNs in the absence and presence of mecamylamine (all SPNs: $p = 0.075$, n = 13; dSPNs: $p = 0.5$, n = 7; iSPNs: $p = 0.095$, n = 6; SRT). Right: percent change in rheobase current after mecamylamine application. **D.** Voltage responses to subthreshold current injections are not enhanced by mecamylamine ($F_{11,120} = 0.86$ $p = 0.58$; n = 11; two-way ANOVA), though a post-hoc Bonferroni test reveals a significant mecamylamine-induced decrease at 50 pA ($p < 0.05$) and 75 pA ($p < 0.01$) current injections. **E.** AP firing frequencies in response to suprathreshold somatic current injections were unaffected by mecamylamine ($F_{20,231} = 0.43$, $p = 0.99$; n = 12; two-way ANOVA).

Fig 7. nAChR-blockade hyperpolarizes PV-FSI resting membrane potential and reduces the frequency of sIPSCs in SPNs. A. Example recordings of sIPSCs from

SPNs voltage-clamped at +10mV, before and during mecamylamine (10 μM) application. **B.** Mecamylamine significantly enhanced sIPSC frequency in SPNs ($F_{8,108} = 2.607$, $p = 0.012$; n = 13; two-way ANOVA). A post-hoc Bonferroni test revealed that this decrease was limited to low amplitude sIPSCs (20 pA bin: $p < 0.001$; 25 pA bin: $p < 0.01$). **C.** Mecamylamine caused a rightward shift in the cumulative probability distribution of sIPSC interevent intervals in SPNs ($F_{20,252} = 2.10$, $p = 4.7 \cdot 10^{-3}$; n = 13; two-way ANOVA). **D.** Example traces of a PV-FSI before and after wash-in of 1 μM DHβE. **E.** Resting membrane potentials of PV-FSIs before and after wash-in of DHβE (n = 12; $p = 9.8 \cdot 10^{-4}$; SRT).

Fig. 8. Blockade of Ca^{2+}-permeable AMPA receptors, to prevent cortical activation of PV-FSIs and related GINs, mimics and occludes the effect of mecamylamine on SPN spike latency. A. Example of the occlusion of the mecamylamine effect on optogenetic synaptic activation of SPNs by the Ca^{2+}-permeable AMPA receptor antagonist Naspm (100 μM). Distribution of spike latencies (**B**) and ADP amplitude (**C**) in response to application of Naspm followed by mecamylamine show that Naspm significantly shortens the AP latency ($p = 1.22 \cdot 10^{-4}$, n = 14 SPNs, SRT) and enhancement of the ADP amplitude ($p = 1.95 \cdot 10^{-3}$, n = 11 SPNs, SRT). In contrast, the subsequent mecamylamine application fails to further shorten the AP latency ($p = 0.6875$, n = 7 SPNs, SRT) or further enhance the ADP amplitude ($p = 0.625$, n = 4, SRT).

Fig. 9. Proposed model of tonic nAChR-mediated suppression of cortically-driven SPN spike latency. Example CIN and SPN firing patterns shown below; dashed red arrows indicate diminished signaling during CIN pauses; Glu = glutamate.

Supplemental Figure Captions

Fig. 1- figure supplement 1. DhβE mimics the effect of mecamylamine on SPN spike latency and ADP amplitude. A-B. DhβE significantly shortens spike latencies ($p = 7.8 \cdot 10^{-3}$, n = 8 SPNs, SRT) (**A**) and ADP amplitudes ($p = 0.03$, n = 8 SPNs, SRT) (**B**).

Fig. 2- figure supplement 1. MLA does not alter release probablity of excitatory synaptic inputs. A. Example responses of an SPN to paired pulse stimulation (electrical stimuli separated by 50 ms) before and in the presence of MLA (5 μM). **B.** MLA had no effect on the EPSC amplitude evoked by the first paired stimulus (P1) ($p = 0.1475$, $n = 11$, SRT). **C.** MLA had no effect on the PPR (P2/P1, $p > 0.9999$, $n = 11$, SRT).

Fig. 3- figure supplement 1. ChR2 expression mice is not observed in cortical or striatal GABAergic neurons in Thy1-ChR2. A. Confocal images from the sensorimotor cortex, auditory (A1) cortex, striatum and globus pallidus (GP) of a Thy1-ChR2 mouse. Tissue was stained for glutamic acid decarboxylase (GAD) or somatostatin (som); colocalization of ChR2 (green) and GAD or som was not observed. ChR2 expression was observed in a population of GP neurons. **B-C.** Example recordings of a SPN in the presence of the AMPA and NMDA receptor blockers DNQX and D-APV reveal the presence of a small but measurable optogenetically generated monosynaptic IPSC in SPNs from Thy1-ChR2 mice. Arrow indicates compound action current in ChR2-laden axons (Tanimura, Lim et al. 2016) (**B**). This monosynaptic IPSC, however, was insensitive to mecamylamine (glutamate blockers vs mec: $p = 0.578$; glutamate blockers + mec vs GABA receptor blockers: $p = 0.0156$; $n = 7$, SRT) (**C**).

Fig. 6- figure supplement 1. Mecamylamine does not shorten the latency of SPN APs induced by somatic current injection, or alter somatic excitability of SPNs from Thy1-ChR2 mice. A. Latencies of APs induced by rheobase current injection (which induced only a single spike) in a mixed population of SPNs before and in the presence of mecamylamine ($p = 0.4238$, $n = 12$, SRT). **B.** Latencies of the first AP in a train induced by suprathreshold current injection in a mixed population of SPNs before and in the presence of mecamylamine ($p = 0\ 022$, $n = 12$, SRT). **C.** IV curves (mean±sem) of a mixed population of SPNs from Thy1-ChR2 mice are not affected by mecamylamine.

Fig 7- figure supplement 1. nAChR-blockade depolarizes SOM+ interneuron membrane potential. A. Example cell attached recordings of a SOM+ interneuron before and after wash-in of mecamylamine (VC = 0 mV, ACSF in recording electrode). **B.** Firing rate calculated from cell attached recordings before and after mecamylamine (n = 5). **C.** Example whole cell recordings of a SOM+ interneuron before and after wash-in of mecamylamine. AP peaks truncated to highlight changes in average membrane potential. **D.** Firing rate calculated from whole cell recordings before and after mecamylamine (n = 19, p = 0.177, SRT). **E.** Average membrane potential before and after wash-in of mecamylamine (n = 17, p = 0.0004, SRT).

References

Abbondanza, A., I. Ribeiro Bas, M. Modrak, M. Capek, J. Minich, A. Tyshkevich, S. Naser, R. Rangotis, P. Houdek, A. Sumova, S. Dumas, V. Bernard and H. Janickova (2022). "Nicotinic Acetylcholine Receptors Expressed by Striatal Interneurons Inhibit Striatal Activity and Control Striatal-Dependent Behaviors." The Journal of Neuroscience **42**(13): 2786-2803.

Abudukeyoumu, N., T. Hernandez-Flores, M. Garcia-Munoz and G. W. Arbuthnott (2019). "Cholinergic modulation of striatal microcircuits." Eur J Neurosci **49**(5): 604-622.

Aceves Buendia, J. J., L. Tiroshi, W. H. Chiu and J. A. Goldberg (2019). "Selective remodeling of glutamatergic transmission to striatal cholinergic interneurons after dopamine depletion." Eur J Neurosci **49**(6): 824-833.

Ade, K., Y. Wan, M. Chen, B. Gloss and N. Calakos (2011). "An Improved BAC Transgenic Fluorescent Reporter Line for Sensitive and Specific Identification of Striatonigral Medium Spiny Neurons." Frontiers in Systems Neuroscience **5**(32).

Akins, P. T., D. J. Surmeier and S. T. Kitai (1990). "Muscarinic modulation of a transient K+ conductance in rat neostriatal neurons." Nature **344**(6263): 240-242.

Albuquerque, E. X., E. F. Pereira, M. Alkondon and S. W. Rogers (2009). "Mammalian nicotinic acetylcholine receptors: from structure to function." Physiol Rev **89**(1): 73-120.

Aosaki, T., M. Kimura and A. M. Graybiel (1995). "Temporal and spatial characteristics of tonically active neurons of the primate's striatum." J Neurophysiol **73**(3): 1234-1252.

Aosaki, T., H. Tsubokawa, A. Ishida, K. Watanabe, A. M. Graybiel and M. Kimura (1994). "Responses of tonically active neurons in the primate's striatum undergo systematic changes during behavioral sensorimotor conditioning." J Neurosci **14**(6): 3969-3984.

Apicella, P. (2017). "The role of the intrinsic cholinergic system of the striatum: What have we learned from TAN recordings in behaving animals?" Neuroscience **360**: 81-94.

Apicella, P., E. Legallet and E. Trouche (1997). "Responses of tonically discharging neurons in the monkey striatum to primary rewards delivered during different behavioral states." Exp Brain Res **116**(3): 456-466.

Arenkiel, B. R., J. Peca, I. G. Davison, C. Feliciano, K. Deisseroth, G. J. Augustine, M. D. Ehlers and G. Feng (2007). "In vivo light-induced activation of neural circuitry in transgenic mice expressing channelrhodopsin-2." Neuron **54**(2): 205-218.

Assous, M. (2021). "Striatal cholinergic transmission. Focus on nicotinic receptors' influence in striatal circuits." Eur J Neurosci **53**(8): 2421-2442.

Assous, M., J. Kaminer, F. Shah, A. Garg, T. Koós and J. M. Tepper (2017). "Differential processing of thalamic information via distinct striatal interneuron circuits." Nat Commun **8**: 15860.

Assous, M. and J. M. Tepper (2019). "Excitatory extrinsic afferents to striatal interneurons and interactions with striatal microcircuitry." Eur J Neurosci **49**(5): 593-603.

Bennett, B. D. and C. J. Wilson (1999). "Spontaneous activity of neostriatal cholinergic interneurons in vitro." J Neurosci **19**(13): 5586-5596.

Bradfield, L. A., J. Bertran-Gonzalez, B. Chieng and B. W. Balleine (2013). "The thalamostriatal pathway and cholinergic control of goal-directed action: interlacing new with existing learning in the striatum." Neuron **79**(1): 153-166.

Brimblecombe, K. R. and S. J. Cragg (2017). "The Striosome and Matrix Compartments of the Striatum: A Path through the Labyrinth from Neurochemistry toward Function." ACS Chem Neurosci **8**(2): 235-242.

Cachope, R., Y. Mateo, B. N. Mathur, J. Irving, H. L. Wang, M. Morales, D. M. Lovinger and J. F. Cheer (2012). "Selective activation of cholinergic interneurons enhances accumbal phasic dopamine release: setting the tone for reward processing." Cell Rep **2**(1): 33-41.

Calabresi, P., D. Centonze, P. Gubellini and G. Bernardi (1999). "Activation of M1-like muscarinic receptors is required for the induction of corticostriatal LTP." Neuropharmacology **38**(2): 323-326.

Contant, C., D. Umbriaco, S. Garcia, K. C. Watkins and L. Descarries (1996). "Ultrastructural characterization of the acetylcholine innervation in adult rat neostriatum." Neuroscience **71**(4): 937-947.

Crittenden, J. R., C. J. Lacey, F. J. Weng, C. E. Garrison, D. J. Gibson, Y. Lin and A. M. Graybiel (2017). "Striatal Cholinergic Interneurons Modulate Spike-Timing in Striosomes and Matrix by an Amphetamine-Sensitive Mechanism." Front Neuroanat **11**: 20.

Dautan, D., I. Huerta-Ocampo, N. K. Gut, M. Valencia, K. Kondabolu, Y. Kim, T. V. Gerdjikov and J. Mena-Segovia (2020). "Cholinergic midbrain afferents modulate striatal circuits and shape encoding of action strategies." Nature Communications **11**(1): 1739.

Day, M., D. Wokosin, J. L. Plotkin, X. Tian and D. J. Surmeier (2008). "Differential excitability and modulation of striatal medium spiny neuron dendrites." J Neurosci **28**(45): 11603-11614.

DiFiglia, M. (1987). "Synaptic organization of cholinergic neurons in the monkey neostriatum." J Comp Neurol **255**(2): 245-258.

Dorst, M. C., A. Tokarska, M. Zhou, K. Lee, S. Stagkourakis, C. Broberger, S. Masmanidis and G. Silberberg (2020). "Polysynaptic inhibition between striatal cholinergic interneurons shapes their network activity patterns in a dopamine-dependent manner." Nat Commun **11**(1): 5113.

Ebihara, K., K. Yamamoto, K. Ueda, N. Koshikawa and M. Kobayashi (2013). "Cholinergic interneurons suppress action potential initiation of medium spiny neurons in rat nucleus accumbens shell." Neuroscience **236**: 332-344.

Elghaba, R., N. Vautrelle and E. Bracci (2016). "Mutual Control of Cholinergic and Low-Threshold Spike Interneurons in the Striatum." Frontiers in Cellular Neuroscience **10**(111).

English, D. F., O. Ibanez-Sandoval, E. Stark, F. Tecuapetla, G. Buzsáki, K. Deisseroth, J. M. Tepper and T. Koos (2011). "GABAergic circuits mediate the reinforcement-related signals of striatal cholinergic interneurons." Nat Neurosci **15**(1): 123-130.

Faust, T. W., M. Assous, F. Shah, J. M. Tepper and T. Koós (2015). "Novel fast adapting interneurons mediate cholinergic-induced fast GABAA inhibitory postsynaptic currents in striatal spiny neurons." Eur J Neurosci **42**(2): 1764-1774.

Faust, T. W., M. Assous, J. M. Tepper and T. Koós (2016). "Neostriatal GABAergic Interneurons Mediate Cholinergic Inhibition of Spiny Projection Neurons." J Neurosci **36**(36): 9505-9511.

Flores-Barrera, E., B. Vizcarra-Chacón, D. Tapia, J. Bargas and E. Galarraga (2010). "Different corticostriatal integration in spiny projection neurons from direct and indirect pathways." Frontiers in Systems Neuroscience **4**.

Gabel, L. A. and E. S. Nisenbaum (1999). "Muscarinic receptors differentially modulate the persistent potassium current in striatal spiny projection neurons." J Neurophysiol **81**(3): 1418-1423.

Gerfen, C. R. and D. J. Surmeier (2011). "Modulation of striatal projection systems by dopamine." Annu Rev Neurosci **34**: 441-466.

Gertler, T. S., C. S. Chan and D. J. Surmeier (2008). "Dichotomous Anatomical Properties of Adult Striatal Medium Spiny Neurons." The Journal of Neuroscience **28**(43): 10814-10824.

Gittis, A. H., D. K. Leventhal, B. A. Fensterheim, J. R. Pettibone, J. D. Berke and A. C. Kreitzer (2011). "Selective Inhibition of Striatal Fast-Spiking Interneurons Causes Dyskinesias." The Journal of Neuroscience **31**(44): 15727-15731.

Gittis, A. H., A. B. Nelson, M. T. Thwin, J. J. Palop and A. C. Kreitzer (2010). "Distinct Roles of GABAergic Interneurons in the Regulation of Striatal Output Pathways." The Journal of Neuroscience **30**(6): 2223-2234.

Goldberg, J. A., J. B. Ding and D. J. Surmeier (2012). "Muscarinic modulation of striatal function and circuitry." Handb Exp Pharmacol(208): 223-241.

Goldberg, J. A. and J. N. Reynolds (2011). "Spontaneous firing and evoked pauses in the tonically active cholinergic interneurons of the striatum." Neuroscience **198**: 27-43.

Graybiel, A. M. and C. W. Ragsdale, Jr. (1978). "Histochemically distinct compartments in the striatum of human, monkeys, and cat demonstrated by acetylthiocholinesterase staining." Proc Natl Acad Sci U S A **75**(11): 5723-5726.

Gustafson, N., E. Gireesh-Dharmaraj, U. Czubayko, K. T. Blackwell and D. Plenz (2006). "A Comparative Voltage and Current-Clamp Analysis of Feedback and Feedforward Synaptic Transmission in the Striatal Microcircuit In Vitro." Journal of Neurophysiology **95**(2): 737-752.

Hao, J. and T. G. Oertner (2012). "Depolarization gates spine calcium transients and spike-timing-dependent potentiation." Curr Opin Neurobiol **22**(3): 509-515.

Higgs, M. H. and C. J. Wilson (2017). "Measurement of phase resetting curves using optogenetic barrage stimuli." J Neurosci Methods **289**: 23-30.

Ibáñez-Sandoval, O., H. S. Xenias, J. M. Tepper and T. Koós (2015). "Dopaminergic and cholinergic modulation of striatal tyrosine hydroxylase interneurons." Neuropharmacology **95**: 468-476.

Johansson, Y. and G. Silberberg (2020). "The Functional Organization of Cortical and Thalamic Inputs onto Five Types of Striatal Neurons Is Determined by Source and Target Cell Identities." Cell Reports **30**(4): 1178-1194.e1173.

Kimura, M., J. Rajkowski and E. Evarts (1984). "Tonically discharging putamen neurons exhibit set-dependent responses." Proc Natl Acad Sci U S A **81**(15): 4998-5001.

Koós, T. and J. M. Tepper (1999). "Inhibitory control of neostriatal projection neurons by GABAergic interneurons." Nature Neuroscience **2**(5): 467-472.

Koós, T. and J. M. Tepper (2002). "Dual cholinergic control of fast-spiking interneurons in the neostriatum." J Neurosci **22**(2): 529-535.

Lapper, S. R. and J. P. Bolam (1992). "Input from the frontal cortex and the parafascicular nucleus to cholinergic interneurons in the dorsal striatum of the rat." Neuroscience **51**(3): 533-545.

Licheri, V., O. Lagström, A. Lotfi, M. H. Patton, H. Wigström, B. Mathur and L. Adermark (2018). "Complex Control of Striatal Neurotransmission by Nicotinic Acetylcholine Receptors via Excitatory Inputs onto Medium Spiny Neurons." J Neurosci **38**(29): 6597-6607.

Liu, C., X. Cai, A. Ritzau-Jost, P. F. Kramer, Y. Li, Z. M. Khaliq, S. Hallermann and P. S. Kaeser (2022). "An action potential initiation mechanism in distal axons for the control of dopamine release." Science **375**(6587): 1378-1385.

Luo, R., M. J. Janssen, J. G. Partridge and S. Vicini (2013). "Direct and GABA-mediated indirect effects of nicotinic ACh receptor agonists on striatal neurones." The Journal of Physiology **591**(1): 203-217.

Mamaligas, A. A., K. Barcomb and C. P. Ford (2019). "Cholinergic Transmission at Muscarinic Synapses in the Striatum Is Driven Equally by Cortical and Thalamic Inputs." Cell Rep **28**(4): 1003-1014.e1003.

Mesulam, M. M., D. Mash, L. Hersh, M. Bothwell and C. Geula (1992). "Cholinergic innervation of the human striatum, globus pallidus, subthalamic nucleus, substantia nigra, and red nucleus." J Comp Neurol **323**(2): 252-268.

Morgenstern, N. A., A. F. Isidro, I. Israely and R. M. Costa (2022). "Pyramidal tract neurons drive amplification of excitatory inputs to striatum through cholinergic interneurons." Sci Adv **8**(6): eabh4315.

Morris, G., D. Arkadir, A. Nevet, E. Vaadia and H. Bergman (2004). "Coincident but distinct messages of midbrain dopamine and striatal tonically active neurons." Neuron **43**(1): 133-143.

Muñoz-Manchado, A. B., C. Bengtsson Gonzales, A. Zeisel, H. Munguba, B. Bekkouche, N. G. Skene, P. Lönnerberg, J. Ryge, K. D. Harris, S. Linnarsson and J. Hjerling-Leffler (2018). "Diversity of Interneurons in the Dorsal Striatum Revealed by Single-Cell RNA Sequencing and PatchSeq." Cell Rep **24**(8): 2179-2190.e2177.

Muñoz-Manchado, A. B., C. Foldi, S. Szydlowski, L. Sjulson, M. Farries, C. Wilson, G. Silberberg and J. Hjerling-Leffler (2014). "Novel Striatal GABAergic Interneuron Populations Labeled in the 5HT3aEGFP Mouse." Cerebral Cortex **26**(1): 96-105.

Nelson, A. B., T. G. Bussert, A. C. Kreitzer and R. P. Seal (2014). "Striatal cholinergic neurotransmission requires VGLUT3." J Neurosci **34**(26): 8772-8777.

Nelson, Alexandra B., N. Hammack, Cindy F. Yang, Nirao M. Shah, Rebecca P. Seal and Anatol C. Kreitzer (2014). "Striatal Cholinergic Interneurons Drive GABA Release from Dopamine Terminals." Neuron **82**(1): 63-70.

Pakhotin, P. and E. Bracci (2007). "Cholinergic Interneurons Control the Excitatory Input to the Striatum." The Journal of Neuroscience **27**(2): 391-400.

Pan, W. X., J. Brown and J. T. Dudman (2013). "Neural signals of extinction in the inhibitory microcircuit of the ventral midbrain." Nat Neurosci **16**(1): 71-78.

Pawlak, V. and J. N. Kerr (2008). "Dopamine receptor activation is required for corticostriatal spike-timing-dependent plasticity." J Neurosci **28**(10): 2435-2446.

Planert, H., S. N. Szydlowski, J. J. J. Hjorth, S. Grillner and G. Silberberg (2010). "Dynamics of Synaptic Transmission between Fast-Spiking Interneurons and Striatal Projection Neurons of the Direct and Indirect Pathways." The Journal of Neuroscience **30**(9): 3499-3507.

Plotkin, J. L. and J. A. Goldberg (2019). "Thinking Outside the Box (and Arrow): Current Themes in Striatal Dysfunction in Movement Disorders." Neuroscientist **25**(4): 359-379.

Poppi, L. A., K. T. Ho-Nguyen, A. Shi, C. T. Daut and M. A. Tischfield (2021). "Recurrent Implication of Striatal Cholinergic Interneurons in a Range of Neurodevelopmental, Neurodegenerative, and Neuropsychiatric Disorders." Cells **10**(4).

Prager, E. M. and J. L. Plotkin (2019). "Compartmental function and modulation of the striatum." J Neurosci Res **97**(12): 1503-1514.

Raz, A., A. Feingold, V. Zelanskaya, E. Vaadia and H. Bergman (1996). "Neuronal synchronization of tonically active neurons in the striatum of normal and parkinsonian primates." J Neurophysiol **76**(3): 2083-2088.

Reynolds, J. N. J., R. Avvisati, P. D. Dodson, S. D. Fisher, M. J. Oswald, J. R. Wickens and Y. F. Zhang (2022). "Coincidence of cholinergic pauses, dopaminergic activation and depolarisation of spiny projection neurons drives synaptic plasticity in the striatum." Nat Commun **13**(1): 1296.

Rice, M. E. and S. J. Cragg (2004). "Nicotine amplifies reward-related dopamine signals in striatum." Nat Neurosci **7**(6): 583-584.

Rock, C., H. Zurita, C. Wilson and A. J. Apicella (2016). "An inhibitory corticostriatal pathway." Elife **5**.

Shen, W., M. Flajolet, P. Greengard and D. J. Surmeier (2008). "Dichotomous dopaminergic control of striatal synaptic plasticity." Science **321**(5890): 848-851.

Shuen, J. A., M. Chen, B. Gloss and N. Calakos (2008). "Drd1a-tdTomato BAC Transgenic Mice for Simultaneous Visualization of Medium Spiny Neurons in the Direct and Indirect Pathways of the Basal Ganglia." The Journal of Neuroscience **28**(11): 2681-2685.

Silberberg, G. and J. P. Bolam (2015). "Local and afferent synaptic pathways in the striatal microcircuitry." Curr Opin Neurobiol **33**: 182-187.

Solinas, M., M. Scherma, L. Fattore, J. Stroik, C. Wertheim, G. Tanda, W. Fratta and S. R. Goldberg (2007). "Nicotinic alpha 7 receptors as a new target for treatment of cannabis abuse." J Neurosci **27**(21): 5615-5620.

Stern, E. A., D. Jaeger and C. J. Wilson (1998). "Membrane potential synchrony of simultaneously recorded striatal spiny neurons in vivo." Nature **394**(6692): 475-478.

Tanimura, A., S. A. Lim, J. J. Aceves Buendia, J. A. Goldberg and D. J. Surmeier (2016). "Cholinergic Interneurons Amplify Corticostriatal Synaptic Responses in the Q175 Model of Huntington's Disease." Front Syst Neurosci **10**: 102.

Tepper, J. M. and J. P. Bolam (2004). "Functional diversity and specificity of neostriatal interneurons." Curr Opin Neurobiol **14**(6): 685-692.

Tepper, J. M., T. Koós, O. Ibanez-Sandoval, F. Tecuapetla, T. W. Faust and M. Assous (2018). "Heterogeneity and Diversity of Striatal GABAergic Interneurons: Update 2018." Frontiers in Neuroanatomy **12**(91).

Tepper, J. M., T. Koós and C. J. Wilson (2004). "GABAergic microcircuits in the neostriatum." Trends Neurosci **27**(11): 662-669.

Tepper, J. M., F. Tecuapetla, T. Koós and O. Ibáñez-Sandoval (2010). "Heterogeneity and diversity of striatal GABAergic interneurons." Front Neuroanat **4**: 150.

Thomas, T. M., Y. Smith, A. I. Levey and S. M. Hersch (2000). "Cortical inputs to m2-immunoreactive striatal interneurons in rat and monkey." Synapse **37**(4): 252-261.

Threlfell, S., T. Lalic, N. J. Platt, K. A. Jennings, K. Deisseroth and S. J. Cragg (2012). "Striatal dopamine release is triggered by synchronized activity in cholinergic interneurons." Neuron **75**(1): 58-64.

Tiroshi, L. and J. A. Goldberg (2019). "Population dynamics and entrainment of basal ganglia pacemakers are shaped by their dendritic arbors." PLoS Comput Biol **15**(2): e1006782.

Wilson, C. J. and P. M. Groves (1981). "Spontaneous firing patterns of identified spiny neurons in the rat neostriatum." Brain Res **220**(1): 67-80.

Wilson, C. J., Z. C. Xu, P. C. Emson and C. Feler (1990). "Anatomical and physiological properties of the cortical and thalamic innervations of neostriatal tissue grafts." Prog Brain Res **82**: 417-426.

Witten, I. B., S. C. Lin, M. Brodsky, R. Prakash, I. Diester, P. Anikeeva, V. Gradinaru, C. Ramakrishnan and K. Deisseroth (2010). "Cholinergic interneurons control local circuit activity and cocaine conditioning." Science **330**(6011): 1677-1681.

Zhou, F.-M., C. J. Wilson and J. A. Dani (2002). "Cholinergic interneuron characteristics and nicotinic properties in the striatum." Journal of Neurobiology **53**(4): 590-605.

Zhou, F. M., Y. Liang and J. A. Dani (2001). "Endogenous nicotinic cholinergic activity regulates dopamine release in the striatum." Nat Neurosci **4**(12): 1224-1229.

Zucca, S., A. Zucca, T. Nakano, S. Aoki and J. Wickens (2018). "Pauses in cholinergic interneuron firing exert an inhibitory control on striatal output in vivo." Elife **7**.

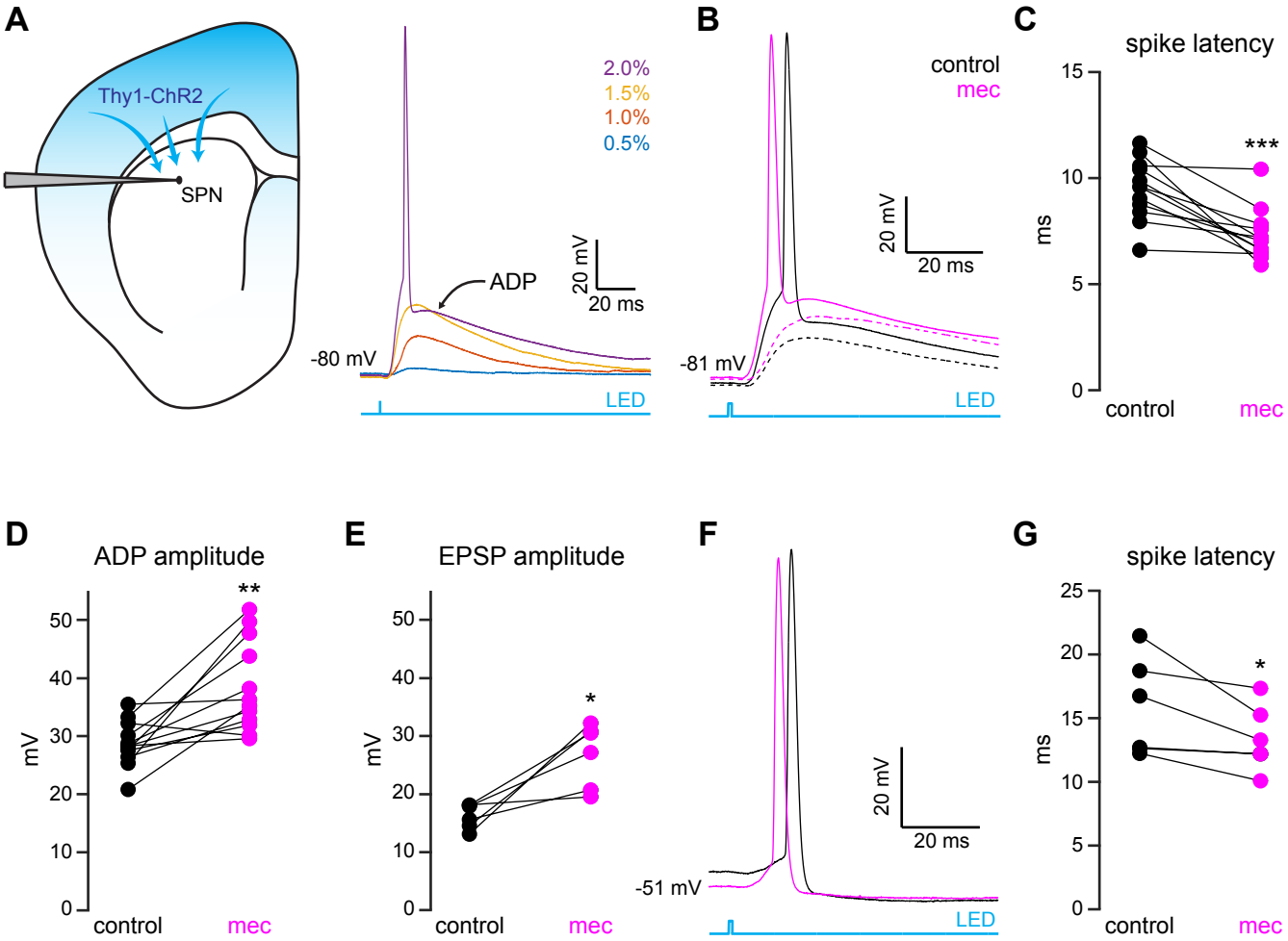
A
Thy1-ChR2
SPN
2.0%
1.5%
1.0%
0.5%
ADP
20 mV
20 ms
-80 mV
LED
B
control
mec
20 mV
20 ms
-81 mV
LED
C
spike latency
15
10
5
0
ms
***
control
mec
D
ADP amplitude
**
50
40
30
20
10
0
mV
control
mec
E
EPSP amplitude
*
50
40
30
20
10
0
mV
control
mec
F
20 mV
20 ms
-51 mV
LED
G
spike latency
25
20
15
10
5
0
ms
*
control
mec

Figure 1

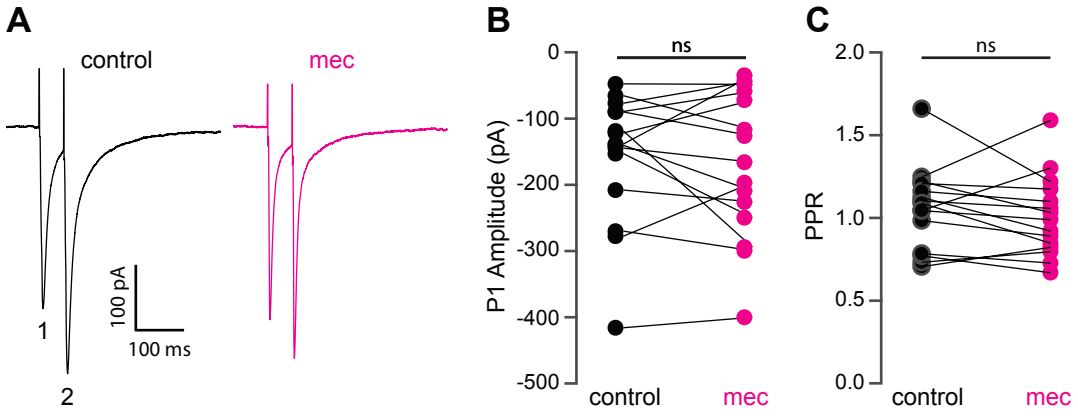
A
control
mec
1
2
100 pA
100 ms
B
ns
P1 Amplitude (pA)
0
-100
-200
-300
-400
-500
control
mec
C
ns
PPR
2.0
1.5
1.0
0.5
0.0
control
mec

Figure 2

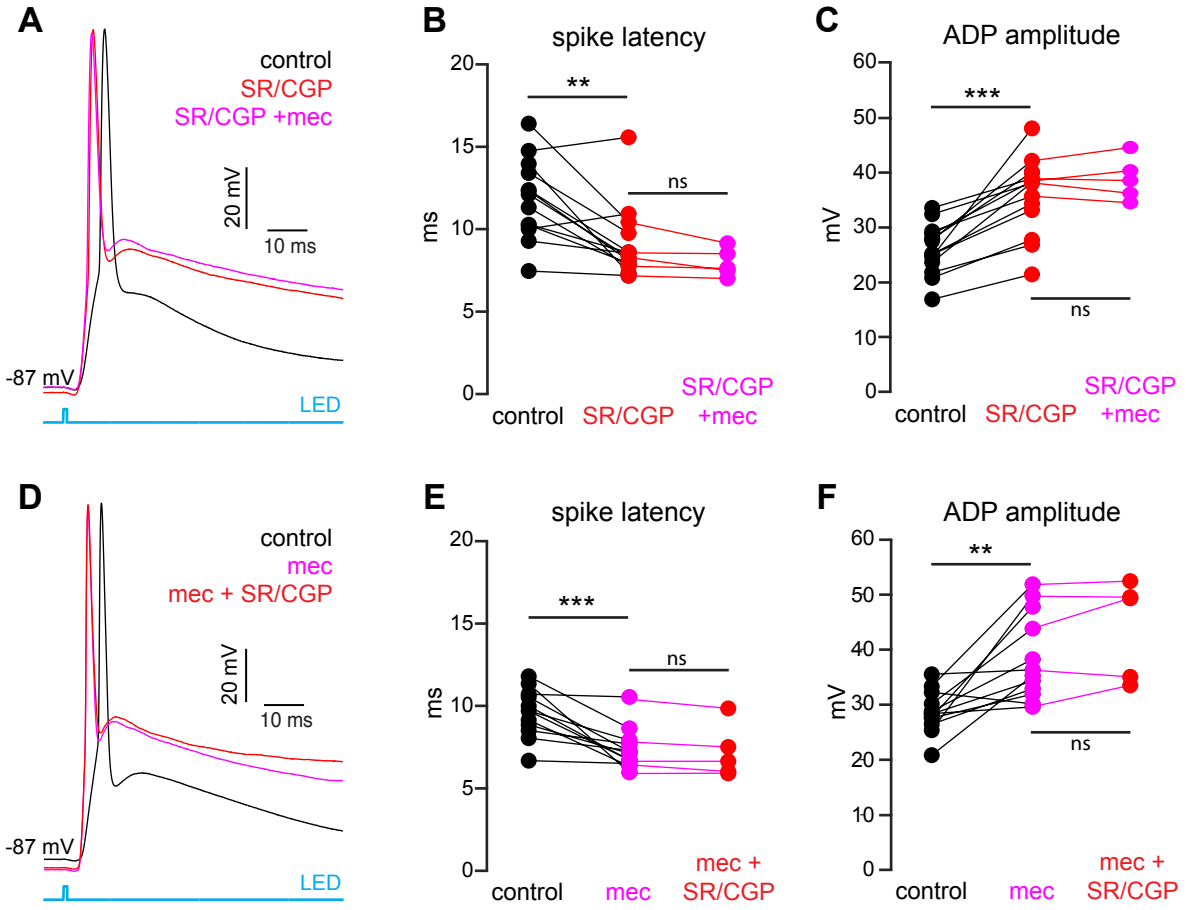
A
control
SR/CGP
SR/CGP +mec
20 mV
10 ms
-87 mV
LED
B
spike latency
ms
20
15
10
5
0
**
ns
control
SR/CGP
SR/CGP +mec
C
ADP amplitude
mV
60
50
40
30
20
10
0
***
ns
control
SR/CGP
SR/CGP +mec
D
control
mec
mec + SR/CGP
20 mV
10 ms
-87 mV
LED
E
spike latency
ms
20
15
10
5
0
***
ns
control
mec
mec + SR/CGP
F
ADP amplitude
mV
60
50
40
30
20
10
0
**
ns
control
mec
mec + SR/CGP

Figure 3

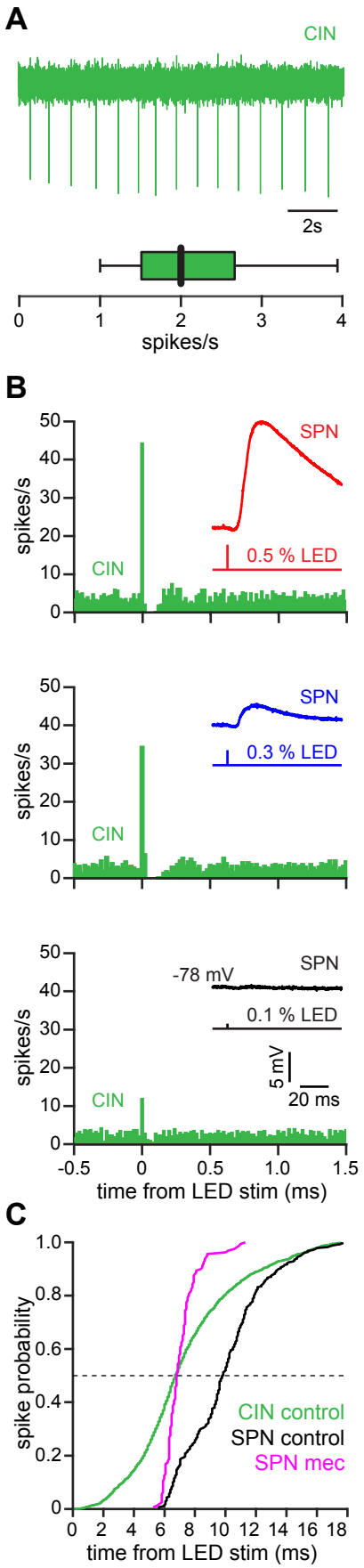
A
CIN
2s
0
1
2
3
4
spikes/s
B
SPN
0.5 % LED
CIN
spikes/s
SPN
0.3 % LED
CIN
spikes/s
SPN
-78 mV
0.1 % LED
5 mV
20 ms
CIN
spikes/s
time from LED stim (ms)
C
spike probability
CIN control
SPN control
SPN mec
time from LED stim (ms)

Figure 4

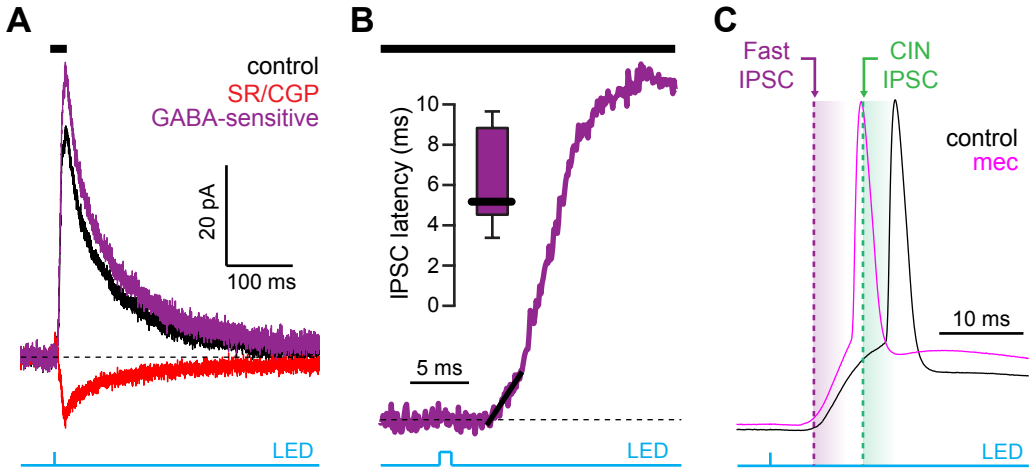
A
control
SR/CGP
GABA-sensitive
20 pA
100 ms
LED
B
IPSC latency (ms)
10
8
6
4
2
0
5 ms
LED
C
Fast
IPSC
CIN
IPSC
control
mec
10 ms
LED

Figure 5

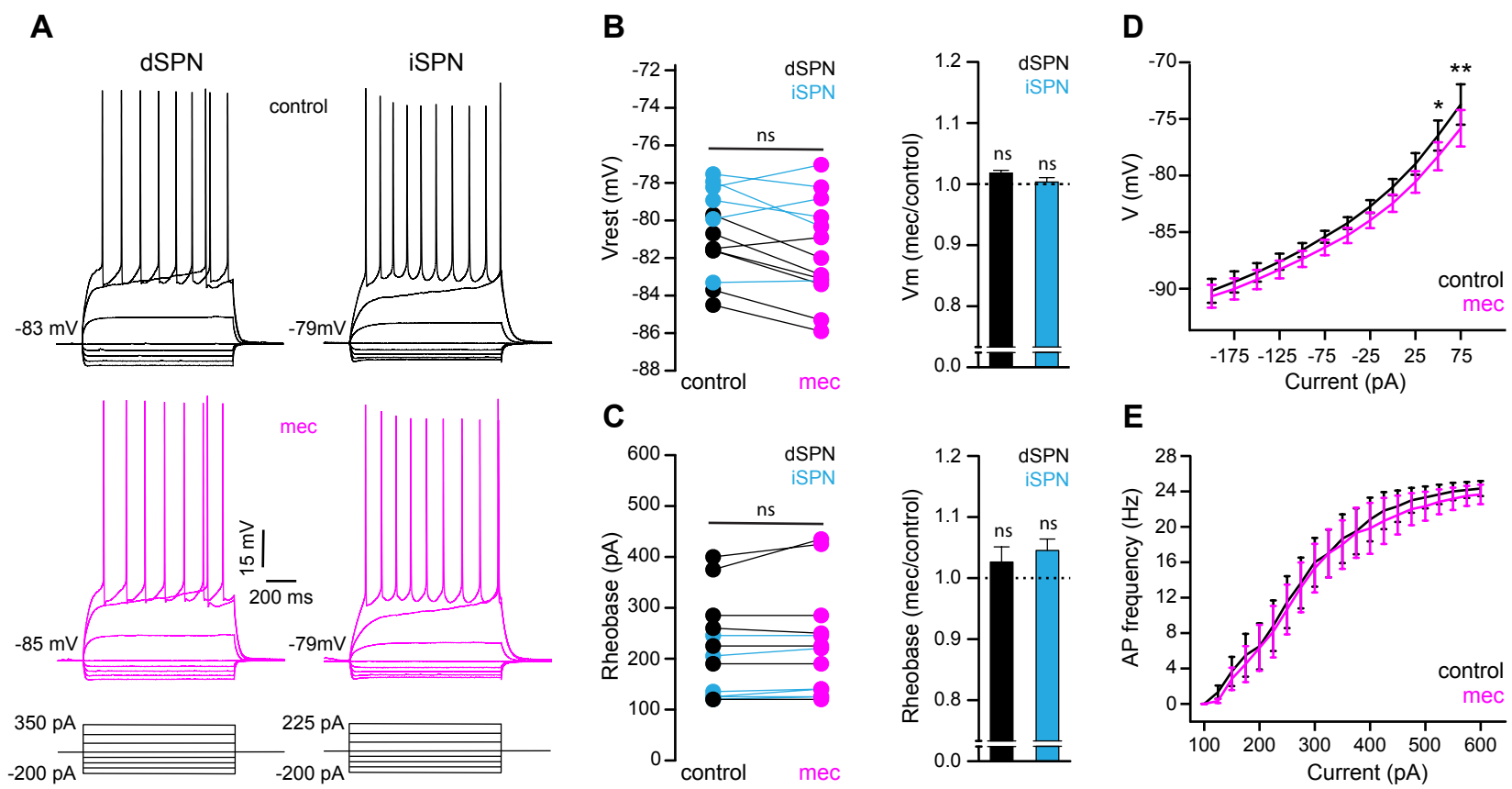
A
dSPN
iSPN
control
-83 mV
-79mV
mec
15 mV
200 ms
-85 mV
-79mV
350 pA
-200 pA
225 pA
-200 pA
B
dSPN
iSPN
Vrest (mV)
ns
control
mec
Vm (mec/control)
ns
ns
C
Rheobase (pA)
Rheobase (mec/control)
D
V (mV)
Current (pA)
control
mec
E
AP frequency (Hz)
Current (pA)

Figure 6

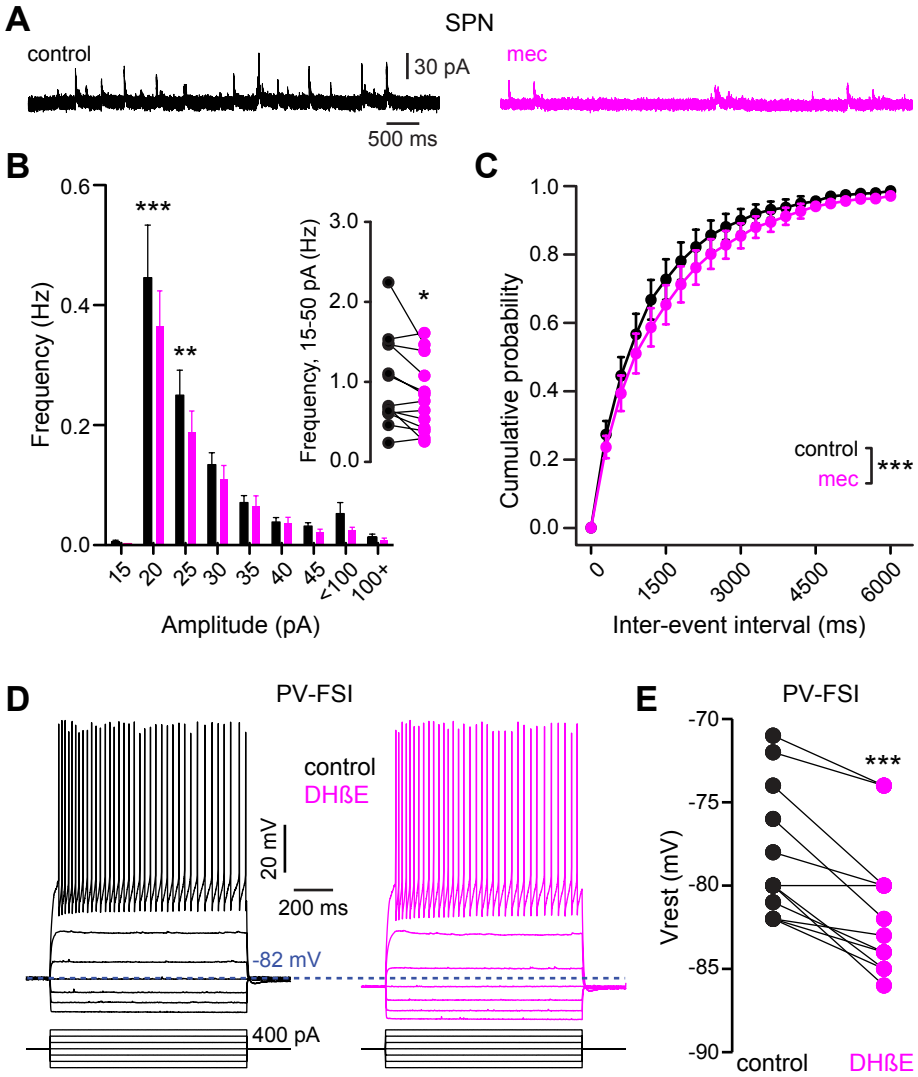
A
SPN
control
30 pA
mec
500 ms
B
Frequency (Hz)
0.6
0.4
0.2
0.0
***
**
15
20
25
30
35
40
45
<100
100+
Amplitude (pA)
Frequency, 15-50 pA (Hz)
3.0
2.0
1.0
0.0
*
C
Cumulative probability
1.0
0.8
0.6
0.4
0.2
0.0
control
mec
***
0
1500
3000
4500
6000
Inter-event interval (ms)
D
PV-FSI
control
DHßE
20 mV
200 ms
-82 mV
400 pA
E
PV-FSI
Vrest (mV)
-70
-75
-80
-85
-90
***
control
DHßE

Figure 7

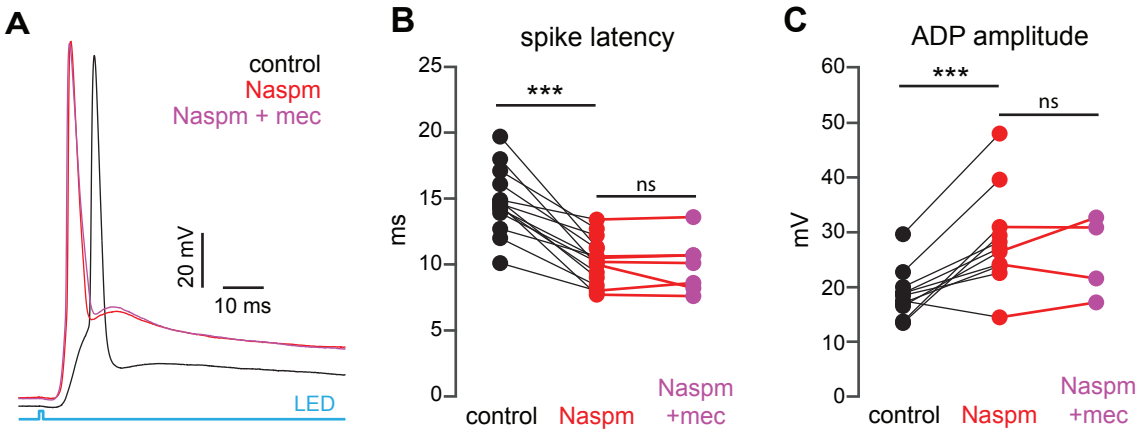
A
control
Naspm
Naspm + mec
20 mV
10 ms
LED
B
spike latency
***
ns
ms
25
20
15
10
5
0
control
Naspm
Naspm
+mec
C
ADP amplitude
***
ns
mV
60
50
40
30
20
10
0
control
Naspm
Naspm
+mec

Figure 8

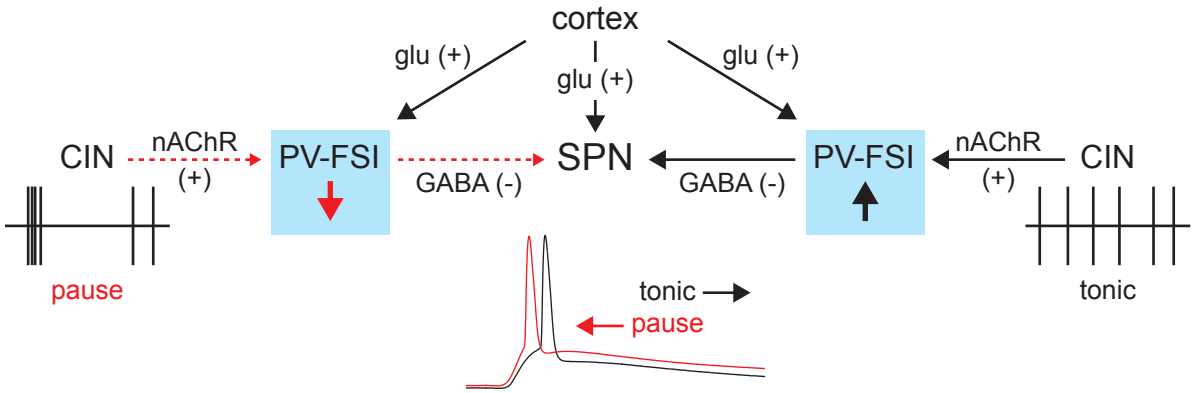
cortex
glu (+)
glu (+)
glu (+)
CIN
nAChR
(+)
PV-FSI
GABA (-)
SPN
GABA (-)
PV-FSI
nAChR
(+)
CIN
pause
tonic
pause
tonic

Figure 9

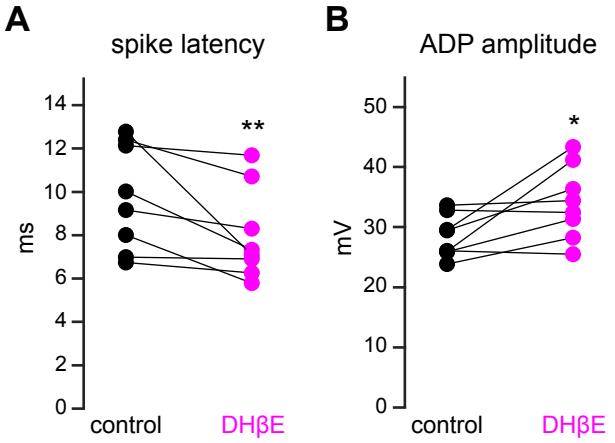

Supp assoc with figure 1

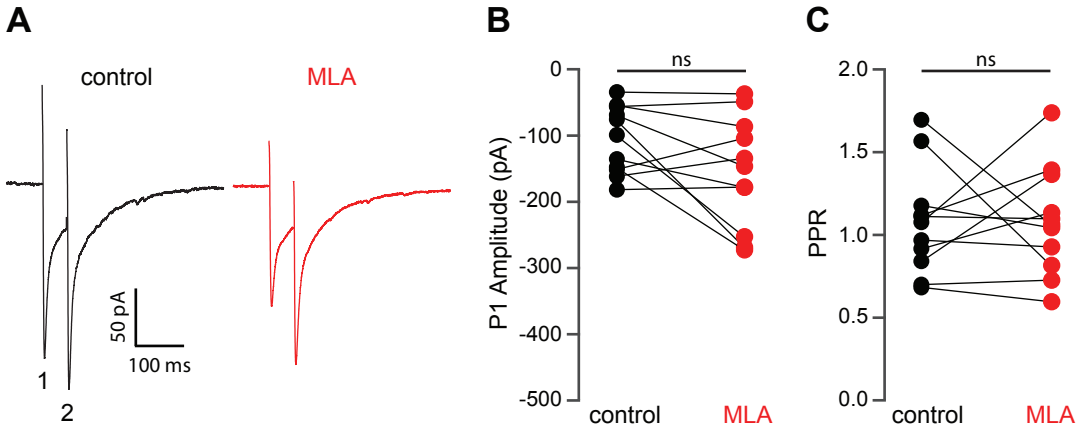

Supp assoc with figure 2

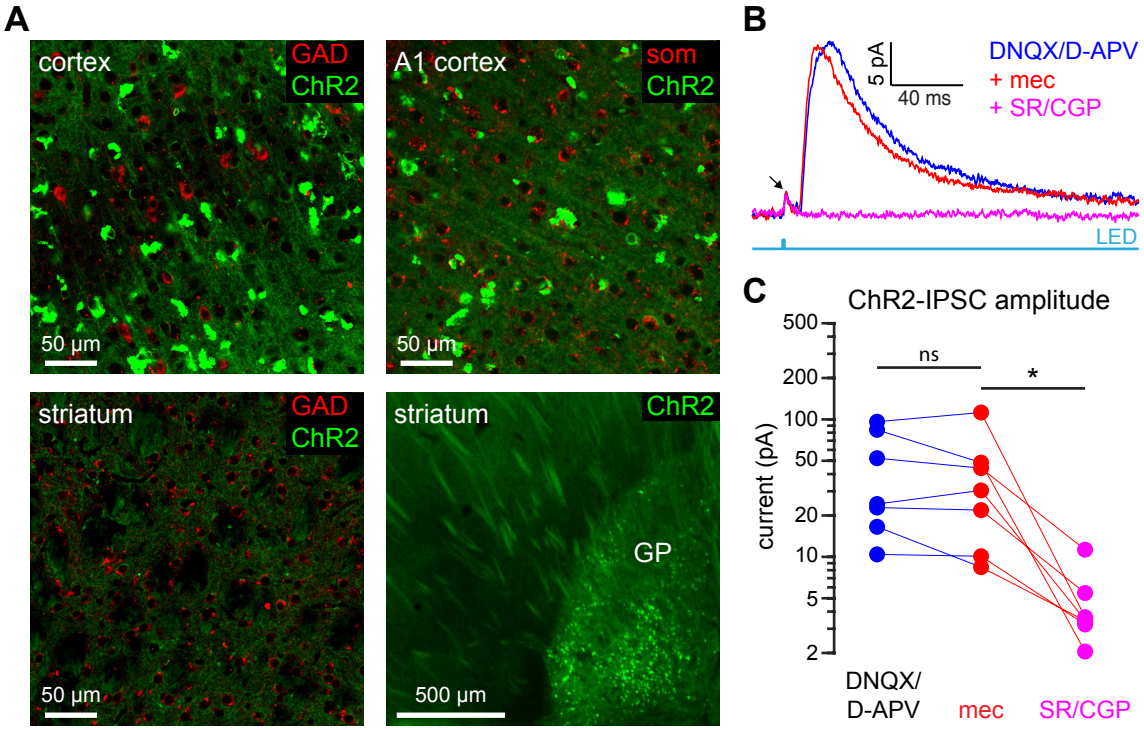

Supp assoc with figure 3

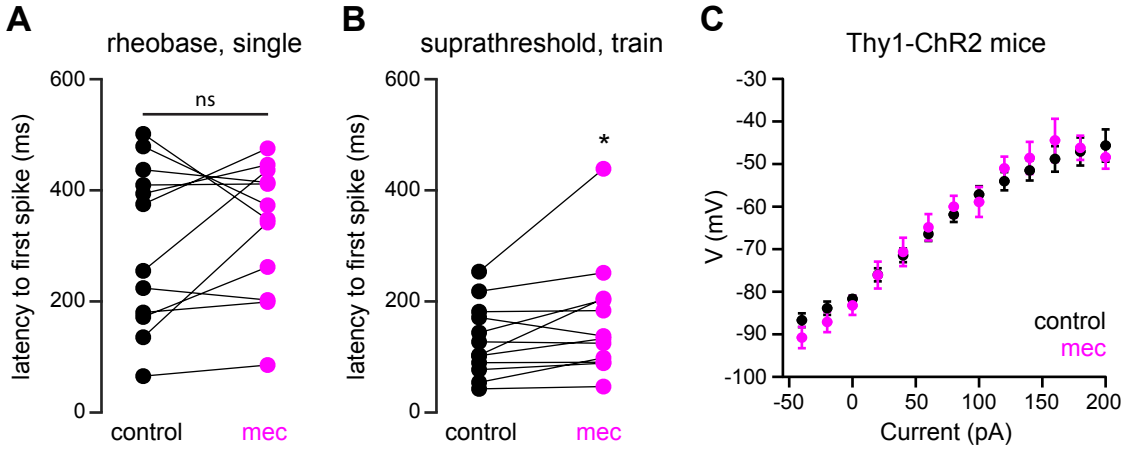

Supp assoc with figure 6

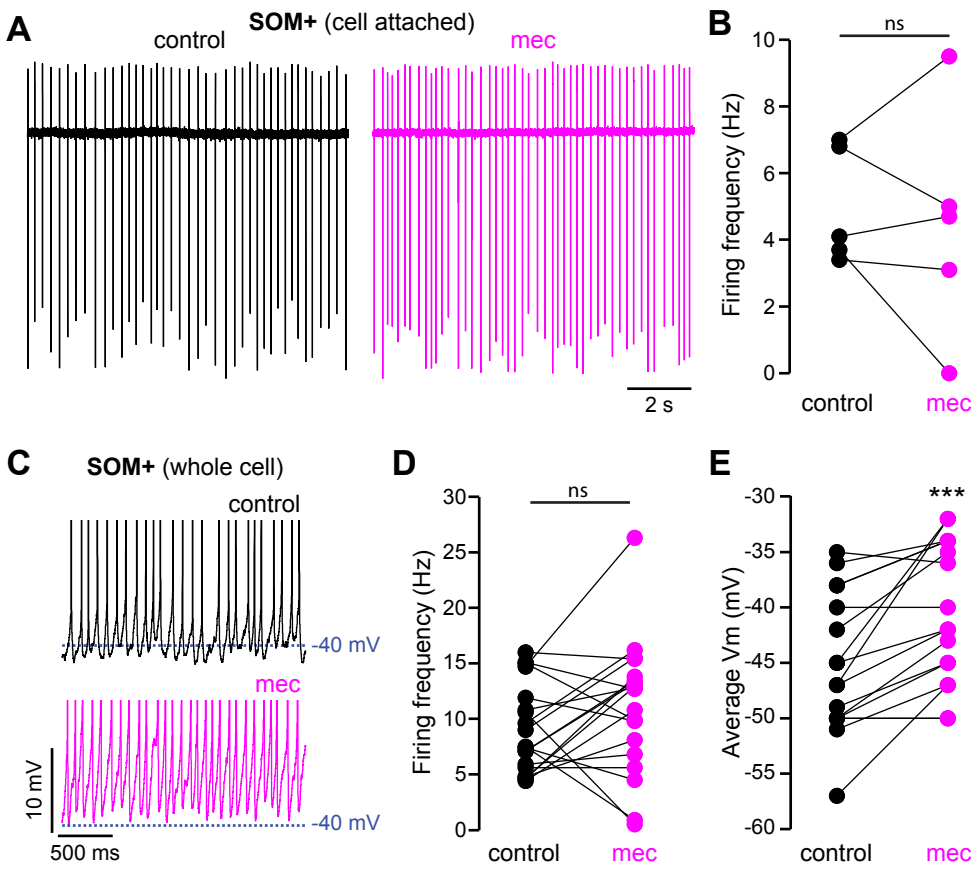

Supp assoc with figure 7